Neurobiology of Language

an open access journal

SPECIAL ISSUE:
The White Matter Connectome Supporting Speech and Language in the Human

Structural Development of Speech Networks in Young Children: A Cross-Sectional Study

Marilyn Curtis[1], Mohammadreza Bayat[1], Dea Garic[2], Alliete R. Alfano[1], Melissa Hernandez[1], Madeline Curzon[1], Andrea Bejarano[1], Pascale Tremblay[3], Shannon Marie Pruden[1], Paulo Graziano[1], and Anthony Steven Dick[1]

[1]Florida International University, Miami, FL, USA
[2]Carolina Institute for Developmental Disabilities, School of Medicine, University of North Carolina at Chapel Hill, Carrboro, NC, USA
[3]Université Laval, Quebec City, Quebec, Canada

Keywords: automated fiber quantification, development, restriction spectrum imaging, speech neurobiology, white matter

ABSTRACT

To investigate speech in the developing brain, 94 children aged 4 to 7 years old were scanned using diffusion weighted imaging (DWI) magnetic resonance imaging. To increase sample size and performance variability, we included children with ADHD from a larger ongoing study (n = 47). Each child completed the Syllable Repetition Task (SRT), a validated measure of phoneme articulation. DWI data were modeled using restriction spectrum imaging to measure restricted and hindered diffusion properties in gray and white matter. We analyzed the diffusion data using whole brain analysis and automated fiber quantification (AFQ) analysis to establish tract profiles for the six fiber pathways thought to be important for supporting speech development. In the whole brain analysis, we found that SRT performance was associated with restricted diffusion in left and right inferior frontal gyrus, left and right pars opercularis, right pre-supplementary and supplementary motor area, and left and right cerebellar gray matter ($p < 0.005$). Age moderated these associations in left pars opercularis and the frontal aslant tract (FAT), but only the cerebellar findings survived a cluster correction. Analyses using AFQ highlighted differences in high and low performing children along specific tract profiles, most notably in left but not right FAT, in left and right superior longitudinal fasciculus III, and in the cerebellar peduncles. These findings suggest that individual differences in speech performance are reflected in structural gray and white matter differences as measured by restricted and hindered diffusion metrics, and offer important insights into developing brain networks supporting speech in very young children.

INTRODUCTION

Contemporary neurobiological models of speech have clarified the primary brain regions and connections that are putatively important for speech. Such models developed in adults are potentially relevant for understanding developing speech in young children, an understudied population with regard to the neurobiology of speech. In fact, very little is known about the development of neural speech pathways in early childhood (i.e., ages 4–8 yr; although see Broce et al., 2015; Chang et al., 2015; Johnson et al., 2022; Liégeois et al., 2019). This highlights a major deficit in our knowledge of the neurobiology of speech development. The

Citation: Curtis, M., Bayat, M., Garic, D., Alfano, A. R., Hernandez, M., Curzon, M., Bejarano, A., Tremblay, P., Pruden, S. M., Graziano, P., & Dick, A. S. (2025). Structural development of speech networks in young children: A cross-sectional study. *Neurobiology of Language*, *6*, nol_a_00168. https://doi.org/10.1162/nol_a_00168

DOI: https://doi.org/10.1162/nol_a_00168

Supporting Information: https://doi.org/10.1162/nol_a_00168

Received: 31 July 2024
Accepted: 24 March 2025

Competing Interests: The authors have declared that no competing interests exist.

Corresponding Author:
Anthony Steven Dick
adick@fiu.edu

Handling Editor:
Kate Watkins

The MIT Press

neurobiological models based on these studies and those in adults allow for some expectation about which brain regions and fiber pathways might be sensitive to individual differences in speech ability as children develop in this age range, but this remains untested. With an understanding of how speech develops in the brain, we can build better developmental models relevant for early disorders of speech production, which is the focus of the present study. In the following sections, we review the relevant brain regions and fiber pathways proposed to support speech production in the developing brain, and the novel diffusion-weighted imaging (DWI) measures we employ to index this development. Further, we discuss the age-appropriate task we use to explore behavioral associations with speech production performance in young children, including those with risk for speech production difficulties, such as children with ADHD.

Brain Regions and Fiber Pathways Supporting Speech Production

The two pertinent contemporary models of speech neurobiology that will frame this investigation—Guenther's GODIVA model (Guenther, 2016) and Hickok's updated model (Hickok et al., 2023)—describe how speech can be construed as a broad, distributed network that includes subcortical and cortical structures, and the white matter pathways which connect them (see Figure 1 for an overview of relevant structures and pathways). According to Guenther, the neural speech network can be parsed into bilateral cortical and subcortical information loops that shape the motor cortical commands for speech (Guenther, 2016). The cortico-basal ganglia loop connects basal ganglia structures (globus pallidus, substantia nigra, caudate, and the putamen) and the ventral lateral nucleus of the thalamus, with various regions of the cerebral cortex, such as the supplementary motor area (SMA) and pre-SMA, the primary motor cortex, the somatosensory cortex, and the premotor cortex (Guenther, 2016). The information loop connecting these subcortical structures plays a key role in the process of selecting and initiating appropriate motor programs for speech (Guenther, 2016). The cortico-cerebellar loop, consisting of projections through the pons, deep cerebellar nuclei, thalamus,

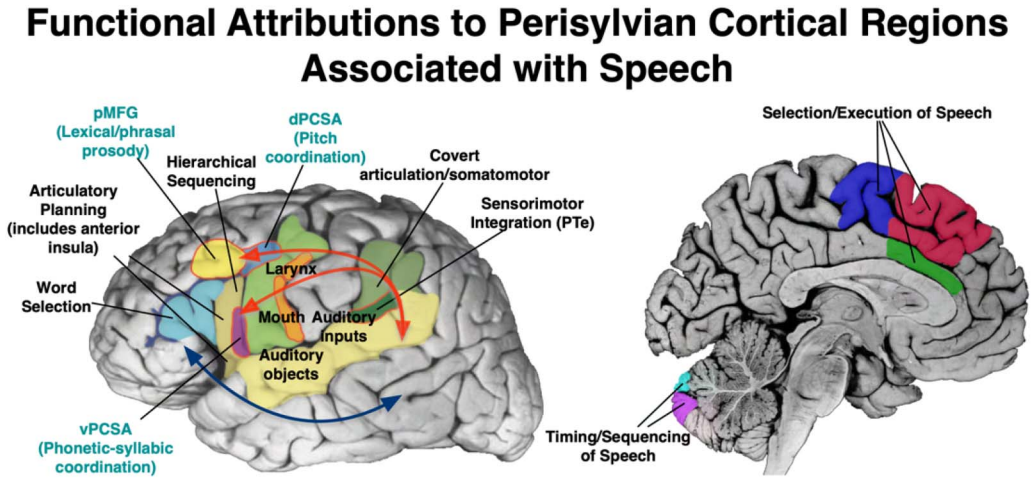

Figure 1. Cortical regions supporting speech are examined in the current study, situated within a broader bilateral but strongly left-lateralized perisylvian language network. The dorsal stream (upper red arrows) is primarily proposed to support sensorimotor speech processing via posterior superior temporal gyrus and sulcus, planum temporale (PTe), and inferior parietal regions (supramarginal gyrus), connecting to inferior frontal and more dorsal premotor regions. Connectivity to pre-supplementary and supplementary motor areas (medial regions in red and blue), basal ganglia (not shown), and cerebellum, rounds out a distributed system supporting speech. The ventral stream (blue arrow) regions primarily support lexical and semantic processing at word, sentence, and narrative levels. pMFG = posterior middle frontal gyrus, dPCSA = dorsal precentral speech area, vPCSA = ventral precentral speech area.

and cerebral cortex, is crucial in the generation of finely timed muscle activations necessary for rapid speech production (Guenther, 2016). The information loops described provide a direct pathway connecting the subcortical structures with the cerebral cortex, where somatosensory and motor representations are integrated, and the motor commands necessary for speech production are generated and initiated.

An extensive cortical model is also presented by Hickok and colleagues (2023). They postulate a model of speech coordination across dual processing streams which integrates primary motor cortical regions, precentral speech areas with prominent roles in speech coordination, and multiple cortical regions necessary for speech production, such as the inferior frontal gyrus (IFG) and superior temporal sulcus (STS). According to this model, speech can be construed as a distributed network across two broad processing streams: the ventral stream, which maps sound onto meaning, and the dorsal stream, which maps sound onto articulatory-based representations (Hickok & Poeppel, 2000, 2004, 2007). The left-dominant dorsal stream has a sensorimotor interface between parietal and temporal regions which projects to an articulatory network in the frontal lobe supporting articulation, specifically involving the posterior IFG (namely pars opercularis), the premotor cortex, and the anterior insula (Hickok & Poeppel, 2007). The bilaterally organized ventral stream is a combinatorial lexical interface implicated in speech recognition, which connects the anterior and posterior regions of the middle temporal gyrus and inferior temporal sulcus (Hickok & Poeppel, 2007), extending beyond the classic left-hemisphere dominant model of speech (Tremblay & Dick, 2016). Evidence from neuroimaging studies has demonstrated an overlap in speech perception and speech production within the superior temporal gyrus (STG), incorporated in both streams (Buchsbaum et al., 2001; Hickok et al., 2003). The dual-stream model expands more simplistic models which envision speech as communication between separate regions controlling speech production and speech perception.

The contributions of the left IFG, neighboring frontal operculum, and insular cortex are emphasized by both Guenther and Hickok and colleagues. Although not addressed by Hickok and colleagues, Guenther additionally emphasizes medial frontal regions associated with motor planning, such as the pre-SMA and SMA. These regions are supported by a monosynaptic pathway known as the frontal aslant tract (Figure 2). The FAT's connectivity of the IFG and pre-SMA/SMA, regions previously associated with motor speech properties (Hertrich et al., 2016), suggests that it may play a role in planning and initiation of speech, especially in the left hemisphere (Dick et al., 2019). Several studies have demonstrated the FAT's association with various aspects of speech, specifically verbal fluency (Catani et al., 2013; Mandelli et al.,

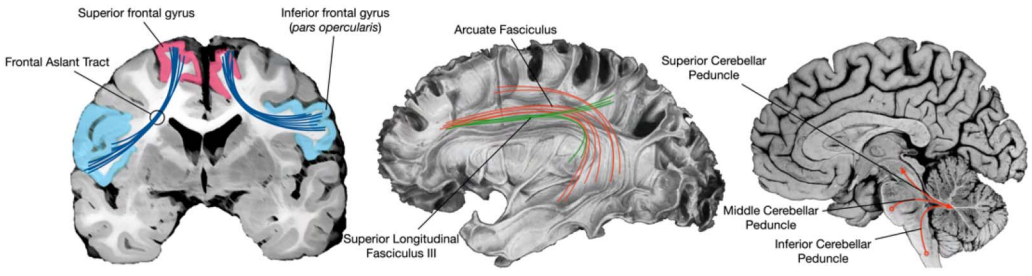

Figure 2. Cortical and cerebellar pathways supporting speech are examined in the current study. The frontal aslant tract connects inferior frontal gyrus and pre-supplementary motor area; superior longitudinal fasciculus III and arcuate fasciculus connect inferior frontal and dorsal premotor cortex with supramarginal gyrus and superior and middle temporal cortex; the three brainstem peduncles support communication with cerebellum.

2014), motor speech initiation (Kinoshita et al., 2015; Zhong et al., 2022), speech fluency impairments such as stuttering (Kemerdere et al., 2016; Kronfeld-Duenias et al., 2016; Misaghi et al., 2018), and speaking rate (Jossinger et al., 2024). Few studies have explored the development of the FAT in young children. For example, Broce and colleagues (2015) tracked the FAT in young children (aged 5–8 yr), but found no associations with phonology and expressive language. One study has linked FAT diffusion properties to stuttering in 6- to 12-year-old children (Misaghi et al., 2018), and another study demonstrated the FAT's association with speech severity in preschool children who have been diagnosed with childhood apraxia of speech (Bombonato et al., 2022). However, no studies, to our knowledge, have examined developmental variability of the FAT in relation to speech in very young children, as we propose to do here.

The left IFG is also a key node in a dorsal pathway for speech (Hickok et al., 2003; Hickok & Poeppel, 2004, 2007; Rauschecker, 1998; Rauschecker & Scott, 2009) mapping sounds onto articulatory-based representations through interactions with the posterior STG and STS (STGp and STSp), planum temporale, and supramarginal gyrus (SMG). The structural connectivity of these regions has been established via several invasive and noninvasive methods (Bernard et al., 2019; Willems et al., 2009). Two major fiber pathways are thought to support dorsal stream connectivity—the superior longitudinal fasciculus III (SLF III) and the arcuate fasciculus (AF). SLF III is thought to support a fronto-parietal articulatory loop implicated in motor speech function, based on disturbances during electrostimulation (Duffau et al., 2003). SLF III is specifically defined by its connectivity with the SMG, involved in processing phonological inputs and outputs (Oberhuber et al., 2016), and IFG and frontal operculum (Bernal & Altman, 2009), thus establishing its putative role in speech production. AF projects more broadly, connecting posterior temporal and inferior parietal cortex with both ventral and superior frontal cortical regions (Barbeau et al., 2020). It has been proposed that the AF plays a role in speech monitoring and motor speech function, due to established connectivity with premotor and primary motor areas in the precentral gyrus (Bernal & Ardila, 2009). Hickok and colleagues have recently delineated a region possibly facilitated by this connectivity, referred to as the dorsal precentral speech area (Hickok et al., 2023). This area has been demonstrated to exert significant influence over prosodic control, an element of speech production. Supporting the claim that SLF and AF play a role in speech production is a study that demonstrated an association with AF and associated segments, including SLF III, and receptive and expressive language in children 5 to 8 years old (Broce et al., 2015), although other research has not found such an association (Morgan et al., 2018). The proposed study seeks to expand on this previous research by focusing on a specific component of speech, phoneme articulation, which will allow us to further parse the specific functions of these support pathways.

The cerebellum and its associated connectivity are also known to support speech, and potentially speech development (Jobson et al., 2024). The involvement of the cerebellum in verbal fluency and articulation tasks is well-established (Riecker et al., 2005, 2006; Schlösser et al., 1998), and anatomical evidence of functional connectivity suggests that the role of the cerebellum may go beyond simple motor generation and activation, as previously thought. As reviewed in Vias and Dick (2017), lateral and medial regions of cerebellar gray matter have been associated with distinct aspects of speech production. Two of the cerebellar lobules that fall along the horizontal cerebellar fissure, Crus I and Crus II, have been shown to play a role in phonological processing through word generation and phonemic and verb fluency tasks (Frings et al., 2006; Schweizer et al., 2010; Stoodley et al., 2012). Activation during fMRI tasks of speech production have revealed findings in the left and right Crus I and Crus II lobules

in adults (Bohland & Guenther, 2006; Correia et al., 2020; Geva et al., 2021; Peeva et al., 2010; Shuster & Lemieux, 2005). In children and adults with FOXP2 mutation, volume reduction in left and right Crus I is correlated with performance on a non-word repetition task (Argyropoulos et al., 2019).

In regard to white matter pathways, the inferior, middle, and superior cerebellar peduncles (ICP, MCP, and SCP) are the three major white matter input and output pathways of the cerebellum (Naidich et al., 2009), linking the lateral cerebellar cortex with subcortical and cortical structures in the cerebral cortex (Vias & Dick, 2017). The right ICP has been linked to developmental differences in children who stutter (Johnson et al., 2022), and, in adults with developmental stuttering, speech rate has been associated with white matter cellular properties of the left ICP (Jossinger et al., 2021). Additionally, white matter properties of the ICP have been correlated with articulation rate, one facet of speech production (Jossinger et al., 2021; Kronfeld-Duenias et al., 2016). In neurotypical adults, the right SCP has been associated with semantic and phonemic verbal fluency, while the right MCP is associated with speaking rate (Jossinger et al., 2024).

Critically, this evidence demonstrates that these distinct cerebellar pathways contribute to elements of speech production beyond articulatory control, such as lexical access (Jossinger et al., 2024). The cerebellum has also been implicated in fine speech control during childhood for children with early speech deficits (Morgan et al., 2011). However, the precise anatomical structures and functional connectivity contributing to such deficits are still unknown. While the cerebellar peduncles and cerebellar gray matter have been established in aspects of speech production, further research is necessary to probe how these regions and pathways are integrated within the broader cortical speech network during development and how this might be moderated by age.

Measurement of White Matter Properties in the Developing Brain

To investigate the development of neural regions and connectivity underlying speech, we examined changes in the microstructural properties of neural and glial cells, as well as their processes (e.g., axons and dendrites). These changes influence the restricted and hindered components of the diffusion signal, which are shaped by cellular properties such as size, density, orientation, and myelination. By leveraging restriction spectrum imaging (RSI) reconstruction, we can separate restricted diffusion from hindered diffusion and free water diffusion (Brunsing et al., 2017; Palmer et al., 2022; White, Leergaard, et al., 2013; White, McDonald, et al., 2013; White et al., 2014).

Restriction spectrum imaging (RSI): Diffusion-weighted imaging reconstruction method that separates restricted, hindered, and free water contributions to the overall diffusion weighted imaging signal.

The restricted diffusion signal reflects water diffusion confined within cell bodies and processes, providing insights into intracellular diffusion properties. In contrast, hindered diffusion captures the characteristics of water navigating the extracellular environment, which constrains molecules to follow more winding or "tortuous" paths in both gray and white matter. Modeling the hindered diffusion signal allows us to better characterize these extracellular properties.

To achieve this level of analysis, we used a specialized multi-shell high-angular-resolution diffusion imaging (HARDI) protocol. This protocol includes both low (b = 500 s/mm^2) and high (b = 3,000 s/mm^2) b-values, robustly sampling the diffusion signal at high b-values. High b-values are especially sensitive to diffusion properties that evolve over longer time intervals. For example, the average diffusion coefficient of restricted intracellular water decreases with diffusion time, but this sensitivity diminishes at lower b-values, where overlap with hindered diffusion becomes more prominent. This combination of advanced acquisition and RSI

reconstruction enables improved separation of hindered and restricted diffusion compared to traditional approaches, such as diffusion tensor imaging (DTI) or single-shell HARDI. It also offers a performance comparable to other multicomponent models, such as Neurite Orientation Density and Dispersion Imaging (NODDI; Zhang et al., 2012).

This methodological foundation enables the indirect measurement of *cellularity*, a term that broadly encompasses the microstructural properties influencing restricted and hindered diffusion signals. While the diffusion signal correlates with these microstructural changes, it is important to note that these properties cannot be directly observed. The restricted diffusion component is expected to increase with processes such as enhanced myelination in both white and gray matter (which reduces extracellular space volume and axonal membrane permeability), increased neurite diameter, dendritic sprouting, or the recruitment and activation of microglia. In contrast, the hindered diffusion component is likely to decrease under the same conditions, reflecting the extracellular environment.

Although these observations are indirect inferences drawn from the diffusion signal, prior research demonstrates that such changes occur in both white and gray matter and can be detected using the proposed diffusion protocol and RSI reconstruction (Palmer et al., 2022). These findings are further supported by histological evidence (White, Leergaard, et al., 2013).

Traditionally, DWI studies have focused on understanding white matter development in specific fiber pathways, or in white matter defined broadly (e.g., via analysis of tract-based spatial statistics). These approaches generally focus on measuring anisotropic diffusion within axons, typically using diffusion-tensor or higher-order spherical deconvolution models. For example, many studies conducting tractography examine fractional anisotropy (FA) differences across age (Lebel et al., 2019), or in association with individual differences in performance on some task (Catani et al., 2013; Dick et al., 2019). An advantage of RSI is that we can measure both white matter tracts and gray matter of the cortex, subcortical structures, and cerebellum (Palmer et al., 2022). While other measures like mean diffusivity are sensitive to differences in gray matter (Sagi et al., 2012), RSI provides a more detailed and biologically specific characterization of tissue properties by distinguishing intra- and extracellular diffusion components. The normalized total signal fractions for restricted (RNT) and hindered (HNT) diffusion produced by this method can be interpreted as reflecting the relative contributions of maturational and developmental cellular processes associated with cell bodies and neurites to diffusion signal in the different compartments. Thus, we can measure the relationship between RSI metrics and cellularity in both gray and white matter structures of the speech network that can be related to individual behavioral differences.

With RSI, we can examine individual differences in both gray and white matter. However, we can also apply more sophisticated analysis to the white matter tracts themselves. We do this in the present study with automated fiber quantification (AFQ; Yeatman et al., 2012). Unlike traditional tractography methods that average across the entire white matter bundle, AFQ segments each tract into 100 equidistant nodes, allowing us to establish a *tract profile* for each child (Yeatman et al., 2012). Thus, we can observe individual differences at specific positions along the tracts, and explore how these individual differences are associated with behavior. For the current analysis, we are interested in white matter pathways associated with the neural speech network, specifically the FAT, AF, SLF III, SCP, MCP, and ICP. We anticipate that these pathways will display differences in measured restricted and hindered diffusion values along the white matter tracts based on speech performance measured by a phoneme articulation task.

Automated fiber quantification (AFQ): Method that segments reconstructed white matter fiber pathways along the length of the pathway so that metrics of diffusion signal can be reported at each segment, rather than for the fiber pathway as a whole.

Variability of Speech Production in Developmental Samples, Including Those at Risk for Speech Delay or Disorder

In the present study, we are interested in examining individual differences in speech production, and their association with structural brain development as measured by diffusion imaging. Examining this relationship requires measured variability in both microstructural properties of the brain and performance on a behavioral task. In order to expand the degree of variability in speech performance, we included as part of the sample children diagnosed with ADHD. This was a practical choice given our data collection of the sample was part of a broader study that included children with ADHD. Importantly, it met two goals: (1) to substantially increase the sample size and statistical power and (2) to increase the variability in performance on the outcome measure of speech production.

The literature provides evidence that children with ADHD are are more likely to display speech production errors than their typically developing peers. For example, children with ADHD are at increased risk for comorbid speech delay (McGrath et al., 2008) and other speech and language impairments (Baker & Cantwell, 1992; Blood et al., 2003; Damico et al., 2010; Donaher & Richels, 2012; Druker et al., 2019; Healey & Reid, 2003), such as specific language impairment. Mueller and Tomblin (Mueller & Tomblin, 2012; Tomblin & Mueller, 2012) reviewed more than 20 studies that evaluated the comorbidity of ADHD and speech and language impairment throughout childhood, finding on average across studies that 50% of children with ADHD are also diagnosed with speech and/or language disorders. In fact, speech, language, and communication difficulties are among the most common comorbid diagnoses for children with ADHD (Mueller & Tomblin, 2012).

Specifically for our purposes, children with ADHD symptoms are more likely to display speech *production* difficulties compared to their typically developing peers (Lee et al., 2017), and they perform more poorly than typically developing children on articulation and phonology tasks (Sarıyer et al., 2023). Thus, we expect that the ADHD group will contribute to the variability in our measure of interest, in addition to increasing the sample size. We also control for ADHD symptomology to ensure that any potential associations with diffusion metrics are not confounded by ADHD symptoms.

The Present Study

The primary aim of the present study is to probe how the neural systems that implement speech develop structurally in children with a wide variety of speech production abilities, including children at risk of speech disorders, such as those with ADHD. A validated measure of phoneme articulation known as the Syllable Repetition Task (SRT) was used to explore the specific role of these regions of interest (ROIs). The SRT is a speech production task suitable for young children with limited phonemic inventories (Shriberg & Lohmeier, 2008; Shriberg et al., 2009), making it an appropriate task to measure speech production errors in young children with and without ADHD. It reliably measures expressive language impairment and auditory-perceptual speech processing errors (Shriberg et al., 2009). The task evaluates pre-articulatory planning, phonological planning, and transformation of phonological plans into motor speech execution (Levelt et al., 1999; Rvachew & Matthews, 2017).

We predict that (1) performance on the SRT will be associated with gray matter cellularity in the cortical and subcortical regions identified to be involved in the neural network of speech; (2) these associations will be moderated by age; and (3) performance on the SRT will

be associated with white matter microstructural properties in the fiber pathways involved with speech speech production, including the FAT, AF, SLF III, and the three cerebellar peduncles.

MATERIALS AND METHODS

Participants

This study is a substudy of a broader research project examining 322 4–7 year olds. That study involved MRI scanning and collection of various behavioral and clinical measures (Table 1). Roughly half of that broader study sample had a diagnosis of ADHD. For this substudy, 113 children also completed the SRT outside the MRI scanner (the COVID-19 pandemic prohibited continued data collection of this particular measure on the full sample because the head-mounted microphone was a transmission risk). We focus in this substudy on the sample of 113 participants who completed the task.

Of the 113 participants who completed the SRT, 10 participants were excluded based on excessive movement (see Image Acquisition), and 9 participants were excluded due to being left-handed (defined by the Edinburgh Handedness Inventory; Oldfield, 1971). Thus, the final analyzed sample size was $n = 94$ ($M_{age} = 5.5$ yr, $SD = 0.82$, 70 males).

Recruitment and eligibility requirements

The study took place in a large urban southeastern city in the U.S. with a large Hispanic/Latino population. Children and their caregivers were recruited from local schools, open houses/parent workshops, mental health agencies, and radio and newspaper ads. Exclusionary criteria for the children included intellectual disability (IQ lower than 70 on the Wechsler Preschool and Primary Scale of Intelligence 4th edition; WPPSI-IV; Wechsler, 2012), confirmed history of autism spectrum disorder, and currently or previously taking psychotropic medication, including children who have been medicated for ADHD. The study was reviewed and approved by the Florida International University Institutional Review Board.

Table 1. Behavioral measures applied for ADHD diagnosis

Measure	Source	Description of measure
Computerized-Diagnostic Interview Schedule for Children (C-DISC)	Shaffer et al., 2000	The C-DISC is a highly structured, computerized diagnostic interview which can be used to assess over 30 different psychiatric disorders, including ADHD. It consists of a series of questions which, after a minimal training period, can be administered by lay interviewers, such as teachers and parents.
Disruptive Behavior Disorders (DBD) rating scale	Graziano et al., 2022; Pelham et al., 1992	The DBD assesses symptoms of ADHD on a four-point scale regarding the frequency of occurrence. For this study, we controlled for hyperactivity/impulsivity and inattention symptoms measured by the DBD to account for ADHD symptomatology.
Impairment Rating Scale (IRS)	Fabiano et al., 2006	The IRS assesses functional impairment in several key domains and can effectively discriminate between children with and without ADHD. Academic, behavioral, and social impairments are measured by a score of three or higher on a seven-point scale.

Note. Dual Ph.D. level clinician review was used to determine diagnosis and eligibility for the sample through assessment of three different measures: the Computerized-Diagnostic Interview Schedule for Children (C-DISC), Disruptive Behavior Disorders (DBD) rating scale, and Impairment Rating Scale (IRS).

Demographics of the sample

Within this subsample, there were 47 typically developing children and 47 children who were diagnosed with ADHD. ADHD diagnosis was accomplished through a combination of parent structured interview (C-DISC; Shaffer et al., 2000) and parent and teacher ratings of symptoms and impairment (Disruptive Behavior Disorders [DBD] rating scale), which involves teacher and parent reporting of symptoms (Fabiano et al., 2006; Graziano et al., 2022), and impairment rating scales (Fabiano et al., 2006). The DBD, updated for DSM-5 terminology (APA, 2013), assesses for symptoms of ADHD, including hyperactivity and impulsivity (Graziano et al., 2022).

Academic, behavioral, and social impairments were measured by a score of three or higher on the seven-point Impairment Rating Scale (Graziano et al., 2022). For this study, ADHD was not considered categorically in our statistical models, but we controlled for ADHD symptoms of inattention and hyperactivity, as measured by the DBD.

The demographic breakdown of the subsample (see Data and Code Availability Statement), which is based on United States National Institutes of Health demographic categories, was: 82% Hispanic/Latino; 87% White; 7% Black; 3% Asian; 3% More than one race. The distribution of maternal education in AHEAD also suggests a good range in our sample catchment: 8.6% of mothers had a high school degree or less, 15.2% had some college, 13.0% had associate's degrees, 25.0% had bachelor's degrees and 38.0% had an advanced degree.

Experimental Paradigm

Children completed an MRI scan and the SRT on the same day, as described below.

Syllable repetition task

The SRT is a child-friendly speech production task that examines expressive speech abilities in individuals with limited phonetic inventories, such as young speakers (Shriberg & Lohmeier, 2008). Research suggests that the SRT is an accurate and stable task for measuring expressive language impairment, as well as auditory-perceptual speech processing errors (Shriberg et al., 2009). The task measures pre-articulatory planning and subsequent planning of articulatory gestures prior to and including motor execution of speech, which includes pre-articulatory encoding and memory of speech sounds, phonological planning, and transforming the phonological plan into a motor plan (Levelt et al., 1999; Rvachew & Matthews, 2017).

During the task, children were asked to repeat a list of 18 two- to four-syllable nonsense words, which were played over computer speakers. The task is available as part of a slide presentation with the audio embedded in each slide, which includes text. The experimenter ensured that the slide presentation was turned away from the participant so that children who could read did not use orthographic information to complete the task. The task starts with simple, two-syllable nonwords such as "ba-da" and increases in difficulty to nonwords such as "ba-na-ma-da." Children were recorded during the task with a head-mounted microphone.

The recordings were independently transcribed and scored by three Spanish-English bilingual research assistants according to the SRT scoring manual, which provided a final percentage score for proportion of correct syllables spoken. Syllable additions, or syllables that the participant produced that were not part of the target word, were tallied. If four or more

responses included syllable additions (25% of items), the score was deemed invalid. In addition, given the large proportion of bilingual Spanish/English speaking children enrolled in our study, and since the SRT was developed for monolingual English-speaking participants, we decided to score the SRT using both the traditional scoring manual as well as a modified bilingual scoring system. The bilingual scoring method modified the traditional scoring method to allow for b/v substitutions, which are two separate phonemes in English but are commonly both pronounced as "b" in Spanish.

Three transcribers, all Spanish-English bilinguals, were trained by a licensed Spanish-English bilingual speech-language pathologist (author A.R.A.). The three transcribers scored according to the bilingual scoring method and had a moderate inter-rater reliability score of $\kappa = 0.587$ (Cohen, 1960). In cases of disagreement, the score for each word was determined by majority (2 out of 3) vote. If agreement could not be reached, the recording was replayed with all transcribers and a licensed Spanish-English bilingual speech-language pathologist present for a final determination. The bilingual scoring was used in the present analysis.

The sample provided a good range of scores on the SRT, providing sufficient variability to examine associations with our brain measures. Performance (percent correct) on the syllable task ranged from 22 to 100, with a mean percentage of 83.67% ($SD = 14.14$; see Figure 3). There was an overall positive effect of age (Figure 3A). As expected, older children performed better on the SRT ($r = 0.25$, $p = 0.015$). We also examined whether there were performance differences between children diagnosed with ADHD and typically developing children. There was no significant performance difference between the groups ($t(92) = -1.20$, $p = 0.23$), so we did not examine the group in the analysis. Instead, as described in the analysis section, we controlled for inattention and hyperactivity symptoms. However, the density plot (Figure 3B) revealed that children with ADHD did contribute scores on the lower end of the performance range, as predicted by literature suggesting children with ADHD display speech production errors. Thus, the inclusion of the ADHD sample did contribute to variability on the measure, and improved the sample size by 100%.

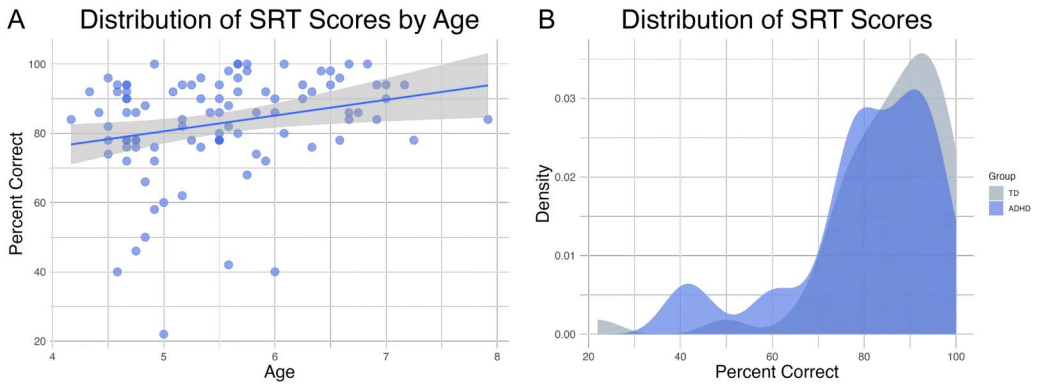

Figure 3. Distribution of Syllable Repetition Task (SRT) scores. (A) Performance by age group. (B) Density plot showing the overall distribution of scores. Both plots display scores as percentage correct using the bilingual scoring system, revealing a good range of performance with some degree of negative skew. Panel A shows a positive effect of age, demonstrating that older children performed better on average. Panel B reveals that while there was no significant difference between groups, children with ADHD did contribute scores on the lower end of the performance spectrum.

Image Acquisition

All imaging was performed using a research-dedicated 3-T Siemens MAGNETOM Prisma MRI scanner (V11C) with a 32-channel coil located on the Florida International University campus. Children first completed a preparatory phase using a realistic mock scanner in the room across the hall from the magnet. Here, they were trained to stay still and were also acclimated to the enclosed space of the magnet, to the back projection visual presentation system and to the scanner noises (in this case, presented with headphones). When they were properly trained and acclimated, they were moved to the magnet. In the magnet, during the structural scans, children watched a child-friendly movie of their choice. Sound was presented through MRI-compatible headphones that also functioned as additional ear protection.

T1-weighted and DWI scans were acquired for each participant. T1-weighted MRI scans were collected using a 3D T1-weighted inversion prepared RF-spoiled gradient echo sequence (axial; TR/TE 2,500/2.88; 1 × 1 × 1 mm, 7 min 12 s acquisition time) with prospective motion correction (Siemens vNav; Tisdall et al., 2012), according to the Adolescent Brain Cognitive Development (ABCD) protocol (Hagler et al., 2019).

Movement artifacts pose challenges for T1-weighted images, which can affect registration in the diffusion scan. Each T1 image was thoroughly reviewed by A.S.D. We applied a visual rating system ranging from *poor* = 1 to *excellent* = 4 for each T1-weighted image, with half-point allowances (e.g., 3.5). Most images were in the 3–4 range, with an average image rating of 3.63 (*SD* = 0.53)

DWI scans were acquired via HARDI with multiband acceleration factor 3 (EPI acquisition; TR/TE = 4,100/88 ms; 1.7 × 1.7 × 1.7 mm; 81 slices no gap; 96 diffusion directions plus 6 b = 0 s/mm^2: b = 0 s/mm^2 [6 dirs], b = 500 s/mm^2 [6-dirs], 1,000 s/mm^2 [15-dirs], 2,000 s/mm^2 [15-dirs] and 3,000 s/mm^2 [60-dirs] s/mm^2; A-to-P direction [7 min 31 s acquisition time]). A second brief scan at b = 0 s/mm^2 in P-to-A direction was acquired to help deal with susceptibility artifacts.

Image postprocessing

DWI preprocessing was performed using a number of complementary software suites. The steps were as follows: (1) outlier detection and replacement, and volume-to-slice correction using a synthetized DWI model, implemented in FSL eddy (Andersson et al., 2016, 2017; note, motion and eddy current distortion correction are implemented in the next step); (2) motion and eddy current distortion correction, implemented with TORTOISE DIFFPREP (Barnett et al., 2014) instead of FSL eddy; (3) creation of a synthesized T2-weighted image from the T1-weighted scan using Synb0-DisCo (Schilling et al., 2019, 2020); (4) correction of spatial and intensity distortions caused by B_0 field inhomogeneity, using TORTOISE DR-BUDDI (Irfanoglu et al., 2015) implementing blip-up/blip-down distortion correction (Andersson et al., 2003; Chang & Fitzpatrick, 1992; Holland et al., 2010; Morgan et al., 2004). This step uses both the reverse-phase encoded b = 0 s/mm^2 image for the estimation of the field map, and the synthesized T2-weighted image for imposition of geometry constraints; (5) gradient nonlinearity correction (gradwarp) using the gradient coefficients supplied by Siemens (Bammer et al., 2003; Barnett et al., 2021; Glover & Pelc, 1986). The outlier-replaced, slice-to-volume registered, transformed for motion, eddy-current corrected, b0-induced susceptibility field corrected, gradient non-linearity corrected images are resampled to the T1-weighted resolution (to 1 mm^3) and registered to the T1-weighted image in a single

interpolation step. For whole brain analysis, data are warped to the ABCD atlas space and reported in LPS atlas coordinates (L = +; P = +; S = +), which are derived from the DICOM coordinate system.

Diffusion Metrics

Restriction spectrum imaging

We took advantage of the multi-shell HARDI acquisition to implement a reconstruction of the diffusion signal with the RSI model (Brunsing et al., 2017; White, Leergaard, et al., 2013; White, McDonald, et al., 2013; White et al., 2014). RSI reconstruction was accomplished in MATLAB using the model from White and colleagues (Brunsing et al., 2017; White, Leergaard, et al., 2013; White, McDonald, et al., 2013; White et al., 2014), and Hagler and colleagues (Hagler et al., 2019), which was updated in Palmer and colleagues (Palmer et al., 2022). The RSI model can be used to quantify the relative proportion of restricted, hindered, and free water diffusion within each voxel of the brain. These components—restricted, hindered, and free water—have intrinsic diffusion characteristics. Free water (e.g., cerebrospinal fluid) is water diffusion unimpeded by tissue structure. In biological tissue, though, the two additional modes of hindered and restricted diffusion predominate (Bihan, 1995). Hindered diffusion describes the behavior of water hindered by the presences of neurites, glia, and other cells, and follows a Guassian displacement pattern. The signal originates from both extracellular and intracellular spaces with dimensions larger than the diffusion length scale (10 μm), and it is affected by the length of the diffusion path by which molecules must travel to navigate cell obstructions. On the other hand, the primary source of restricted diffusion signal in biological tissue comes from cell membranes. Restricted diffusion thus relates to the physical obstruction of molecules within cellular compartments. If the diffusion time Δ is long enough, the length scale of diffusion will vary depending on whether diffusion is hindered or restricted (White, Leergaard, et al., 2013). The acquisition parameters applied in the present study are designed to optimize sensitivity to the different diffusion processes.

A number of quantitative metrics can be recovered from the RSI reconstruction of the diffusion data (Palmer et al., 2022). The model estimates diffusion within different compartments, and provides metrics that are normalized into signal fractions in order to determine the relative proportion of restricted, hindered, and free water diffusion within each voxel. We focus on two metrics—the RNT and the HNT.

The hindered and restricted compartments are modeled as fourth-order spherical harmonic functions, and the free water compartment is modeled using zeroth-order spherical harmonic functions. Axial diffusivity is assumed to be constant at 1×10^{-3} mm^2/s for the restricted and hindered compartments. For the restricted compartment, the radial diffusivity is fixed to 0 mm^2/s. For the hindered compartment, radial diffusivity is fixed to 0.9×10^{-3} mm^2/s. Isotropic diffusivity is fixed to 3×10^{-3} mm^2/s for the free water compartment. Spherical deconvolution is applied to reconstruct the fiber orientation distribution (FOD) in each voxel for the restricted compartment. The norm of the second and fourth order spherical harmonic coefficients is the restricted directional measure (RND; modeling oriented diffusion from multiple directions in a voxel), and the spherical mean of the FOD across all orientations is the restricted isotropic measure (RNI). The sum of RND and RNI is the RNT. (For more details, see Brunsing et al., 2017; Palmer et al., 2022; White, Leergaard, et al., 2013; White, McDonald, et al., 2013; White et al., 2014.)

The two metrics extracted from RSI, RNT, and HNT, can be interpreted as reflecting the relative contributions of maturational and developmental cellular processes associated with

cell bodies and neurites (neural projections from the cell body such as axons and dendrites) to signal in the different compartments. These maturational and developmental processes include myelination, dendritic sprouting, changes in neurite diameter with constant neurite density, changes in cell body size with constant cell density, and changes in the concentration of mature astrocytes. Inspection of the diffusion maps of these metrics, and prior research using the same acquisition parameters in adolescents (Palmer et al., 2022), show that RNT and HNT reliably distinguish white and gray matter and show age-related change in both tissue types (Palmer et al., 2022). The two metrics tend to be anticorrelated. For example, increased myelination is associated with increased restricted diffusion (due to reduced permeability of axonal membranes), and decreased hindered diffusion (due to reduced volume of extracellular space). However, this is not always the case and depends on specific tissue properties and the parcellation of signal within the different diffusion compartments in a voxel.

Data Analysis

Statistical model for fast and efficient mixed-effects algorithm and AFQ analysis

We conducted the statistical analysis using both a fast and efficient mixed-effects algorithm (FEMA; Parekh et al., 2024) and AFQ (Yeatman et al., 2012). FEMA is a voxel-wise whole brain analysis method, and AFQ is designed for specific fiber pathways. These methods are described below. First we detail the statistical models.

The same basic model was run for three analyses: (1) the FEMA model main effect tested, voxel-wise, the association between SRT performance and diffusion metrics; (2) the FEMA model interaction added the interaction term for age and SRT performance, which tests, voxel-wise, where the association between SRT and diffusion metrics are moderated by age; and (3) the AFQ model, which conducts the AFQ analysis to identify where along the specific fiber pathway performance differences are associated with diffusion metrics (by entering the interaction of SRT performance and NodeID). These models are described in Equations 1–6. Models were run with RNT and HNT as outcomes, and with the specified covariates.

FEMA model RNT main effect

$$\text{RNT} \sim \text{SRT performance} + \text{age in months} + \text{sex} + \text{hyperactivity symptoms} + \text{inattention symptoms} + \text{parent education} + \text{motion} + \text{whole brain RNT} + \varepsilon \quad (1)$$

FEMA model HNT main effect

$$\text{HNT} \sim \text{SRT performance} + \text{age in months} + \text{sex} + \text{hyperactivity symptoms} + \text{inattention symptoms} + \text{parent education} + \text{motion} + \text{whole brain HNT} + \varepsilon \quad (2)$$

FEMA model RNT interaction

$$\text{RNT} \sim \text{SRT performance} * \text{age in months} + \text{sex} + \text{hyperactivity symptoms} + \text{inattention symptoms} + \text{parent education} + \text{motion} + \text{whole brain RNT} + \varepsilon \quad (3)$$

FEMA model HNT interaction

$$\text{HNT} \sim \text{SRT performance} * \text{age in months} + \text{sex} + \text{hyperactivity symptoms} + \text{inattention symptoms} + \text{parent education} + \text{motion} + \text{whole brain HNT} + \varepsilon \quad (4)$$

AFQ model RNT

$$\text{RNT} \sim \text{SRT performance} * \text{NodeID} + \text{age in months} + \text{sex} + \text{hyperactivity symptoms} + \text{inattention symptoms} + \text{parent education} + \text{motion} + \text{whole brain RNT} + \varepsilon \quad (5)$$

AFQ model HNT

$$\text{HNT} \sim \text{SRT performance} * \text{NodeID} + \text{age in months} + \text{sex} + \text{hyperactivity symptoms} + \text{inattention symptoms} + \text{parent education} + \text{motion} + \text{whole brain HNT} + \varepsilon \quad (6)$$

Covariates

We included age, sex assigned at birth (sex), parental education, and ADHD symptomatology (inattention and hyperactivity from the DBD (Fabiano et al., 2006; Graziano et al., 2022)) as covariates. Age, sex, and parental education were all parent reported, and the DBD measures also included teacher report. In addition, we included the whole brain diffusion metric (either RNT or HNT). Whole brain diffusion data were output directly from the postprocessing stream to control for general individual differences in diffusion properties of the brain.

Finally, we know participant movement has a substantial effect on DWI measurements, and can introduce spurious group differences in cases where none are present in the biological tissue (Yendiki et al., 2014). Therefore, incorporating movement as a nuisance regressor is recommended (Yendiki et al., 2014). To do this, we estimated movement using the root-mean-square (RMS) output from FSL eddy and implemented an overall movement cutoff for inclusion in analysis. This was arbitrarily defined as average RMS movement of more than one voxel (1.7 mm) over the course of the scan. As noted above, 19 children (6% of the overall sample of $n = 322$) exceeded the movement criteria and were dropped from the sample. For participants retained in the analysis, movement was incorporated as a nuisance regressor in all analyses.

Fast and efficient mixed-effects algorithm

We performed a whole brain, voxel-wise analysis using FEMA. The algorithm is uniquely suited for large sample sizes due to its ability to efficiently perform whole-brain image-wise analyses on complex large scale imaging data (Parekh et al., 2024). It was chosen as an appropriate analysis for the current study because it is optimized for the ABCD brain atlas, and the T1-weighted MRI scans for the current study were collected according to protocol established by the ABCD study (Hagler et al., 2019). The design matrix was constructed to examine the effect of SRT performance on our diffusion metrics of interest, as specified in the statistical models above. The per-voxel threshold was set at $p < 0.005$. For the interaction effect, the same basic results were obtained at $p < 0.001$, so this more stringent threshold is reported for that analysis. In order to apply cluster-mass correction to correct for multiple comparisons, we repeated the analysis using FSL's randomise (note since this is not a multilevel model, the same results are obtained in FSL and FEMA). Both uncorrected and cluster-mass-corrected data are reported.

Automated fiber quantification

Our second analysis allowed us to examine our white matter tracts of interest in-depth via AFQ. The preprocessed DWI images were analyzed by the AFQ software developed by

Yeatman and colleagues (2012), which has since been applied in a number of studies conducted on speech fluency (Jossinger et al., 2021, 2024; Kronfeld-Duenias et al., 2016; Yablonski et al., 2021). Using the AFQ toolbox, we identified and quantified six left and right white matter tracts for analysis: FAT, AF, SLF III, ICP, MCP, and SCP. Parameters followed the AFQ protocol developed by Kruper and colleagues (2021), with the addition of the left and right FAT as described by Kronfeld-Duenias and colleagues (2016).

The implementation of the AFQ software, as described in Yeatman and colleagues (2012), begins with the identification of ROIs. Fiber tracts are identified using a probabilistic streamline tracking algorithm and refined based on waypoint ROIs, which define the trajectory of the fascicle. An iterative procedure cleans the bundles by removing fibers that are more than 4 standard deviations above the mean fiber length or 5 standard deviations from the core of the fiber tract. AFQ software calculates the tract profiles with a vector of one hundred values representing diffusion properties, which have been sampled at equidistant locations along the central portion of the tract.

Automatic segmentation of the FAT and SLF III was carried out using the standard AFQ regions (Yeatman et al., 2012). Upon visual inspection, we established new seed ROIs for the AF based on the long segment definition, as defined in Broce et al. (2015). For the cerebellar peduncles, we used the revised protocol from Jossinger and colleagues (2024). New ROIs defined on the Montreal Neurological Institute (MNI) template were used to identify the peduncles, together with previous ROIs established by Bruckert and colleagues (2019). This method uses probabalistic tractography coupled with constrained spherical deconvolution (CSD) modeling, which has been shown to be more successful in tracking the decussation of the cerebellar peduncles, compared to the traditional deterministic tractography such as that used by Bruckert and colleagues (2019) (see Jossinger et al., 2024). Upon visual inspection of the MCP, we modified the ROIs to remain consistent with established definitions (Jobson et al., 2024; Nagahama et al., 2021).

After running the AFQ analysis, all data were retained for left and right FAT, SLF III, and AF. All participants were retained for left ICP, but for right ICP one participant did not have a complete tract profile. For the left MCP, three participants had incomplete tract profiles, and one participant had an incomplete tract profile for the right MCP. The SCP proved to be the most difficult to track, as 39 participants had incomplete tract profiles (41%) for the left SCP, and 32 participants had incomplete tract profiles (34%) for the right SCP. For all incidents of missingness, we performed deletion of the individual tract profile for that participant. These participants were retained in the whole brain analysis.

From these individual profiles, we created standardized tract profiles by calculating the mean and standard deviation of each diffusion property at each node of each tract, which we then applied to a series of generalized additive models (GAMs). GAMs have been shown to be well suited for modeling diffusion data based on AFQ, since they account for the distribution and noncontinuous nature of diffusion metrics (Muncy et al., 2022). Using this method, we identified nodes which significantly differed in diffusion properties along each white matter tract and related these differences to SRT performance. We compared two different models to determine the best fit: one simple model calculating the main effect of SRT score on the diffusion metrics, and one that took into account the interaction of the nodes, to determine the best model fit for the current analysis. For graphing purposes, we created groups based on a median split. This allowed us to plot how diffusion metrics differed between high and low SRT scores at different node intervals. In the statistical models, SRT was entered as a continuous variable.

Generalized additive model (GAM): Flexible extension of generalized linear model that allows for nonlinear relationships between predictor variables and the response variable. GAMs achieve this by using smoothing functions, such as splines, to model the effects of predictors without assuming a specific parametric form.

RESULTS

Whole Brain Analysis

We first present results for the four voxel-wise FEMA models. For all these models only the cerebellar findings survive correction for multiple comparisons. We report uncorrected findings because several clusters were found in expected regions based on our literature review, so we focus on these clusters. In the Discussion, we consider these findings with this caveat in mind. Regions and pathways are from the ABCD atlas space, using the Destrieux Freesurfer regions (Destrieux et al., 2010) based on the anatomical definitions from Duvernoy (Naidich et al., 2009) and the pathways from Hagler et al. (2009).

Figure 4 and Figure 5 demonstrate the main effect, reporting voxels that show an association between SRT performance and either RNT or HNT. For RNT, uncorrected (Figure 4A) whole brain voxel-wise analysis revealed that speech performance on the SRT task was associated with gray and white matter cellularity in multiple regions, including left and right IFG pars opercularis, right pre-SMA/SMA, FAT white matter, and left and right cerebellum gray and white matter (the cerebellar peduncles). As Figure 4B shows, only the cerebellar clusters survived the cluster correction. For HNT, the same regions were revealed to be associated with SRT performance. However, the cerebellar clusters were smaller, and in fact no clusters survived statistical correction (Figure 4A and B).

Figure 6 and Figure 7 show the results for the interaction effect. These are reported for the more strict $p < 0.001$ threshold, as the cluster-corrected findings were the same for the $p < 0.005$ level. Age moderated the association between SRT and both RNT and HNT in left FAT, left and right caudate, right globus pallidus, and large parts of left and right cerebellum.

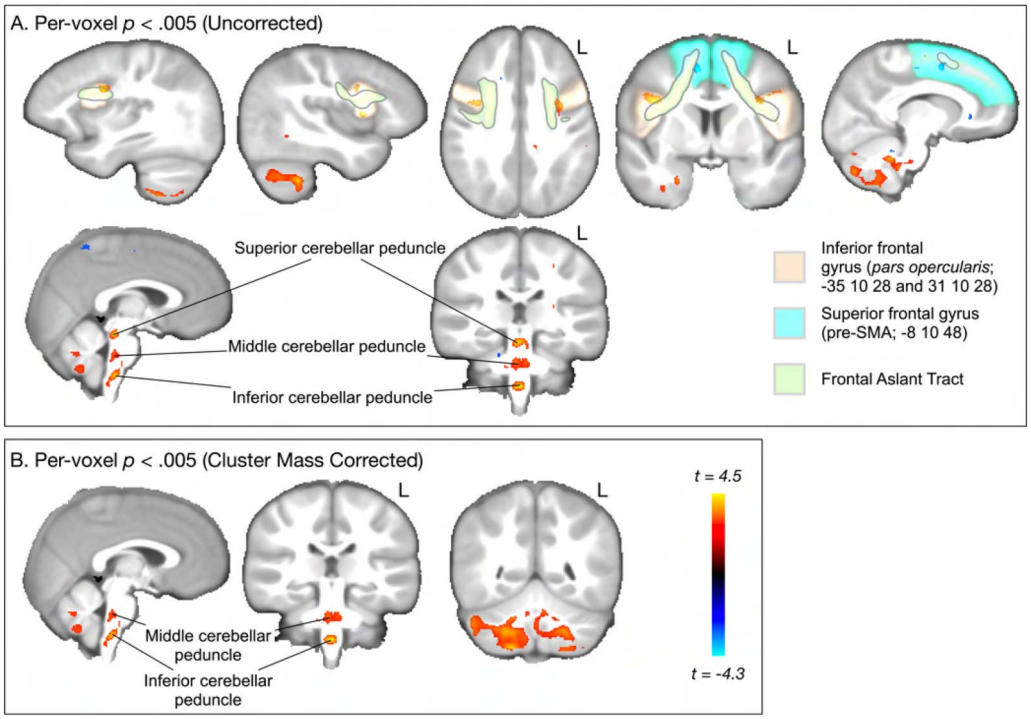

Figure 4. Whole brain, voxelwise analysis of the main effect association between SRT performance and RNT (model Equation 1). (A) Uncorrected ($p < 0.005$) clusters are highlighted for regions and pathways reviewed in the Introduction. Areas in red spectrum indicate a positive association between SRT performance and grey and white matter cellular properties, as measured by RNT. Blue indicates a negative association between SRT performance and RNT. (B) Cluster mass corrected ($p < 0.005$) results show only clusters in cerebellar gray and white matter.

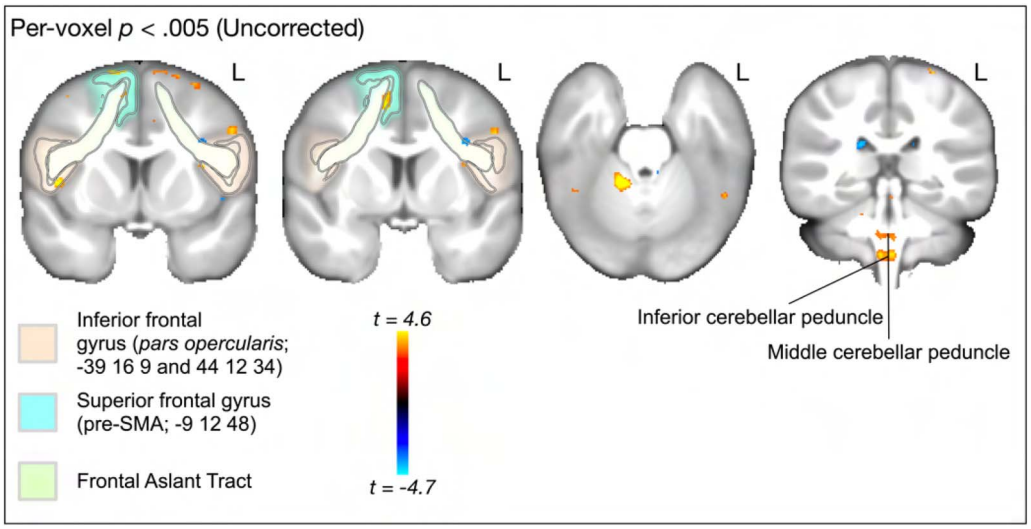

Figure 5. Whole brain, voxel-wise analysis of the main effect association between SRT performance and HNT (model Equation 2). Uncorrected ($p < 0.005$) clusters are highlighted for regions and pathways reviewed in the Introduction. Areas in red spectrum indicate a positive association between SRT performance and gray and white matter cellular properties, as measured by RNT. Blue indicates a negative association between SRT performance and RNT. No voxels in the whole brain analysis survived cluster mass correction ($p < 0.005$). HNT/RNT = hindered/restricted normalized total signal fraction.

For RNT, there was an additional cluster in left pars opercularis. In both RNT and HNT analyses, only the cerebellar clusters survived multiple comparison correction (panel B in both figures). Figure 8 shows the nature of this interaction for the clusters revealed in cerebellum. For RNT, the interaction effect shows that performance is positively associated with RNT, especially for older ages. For HNT, the performance association reduces as age increases.

AFQ Analysis

To further probe the relationship between SRT performance and diffusion metrics along each white matter tract, we examined the tract profiles of white matter pathways identified in our literature review as potentially important for speech. Thus, AFQ analysis was conducted on the FAT, SLF III, AF, ICP, MCP, and SCP.

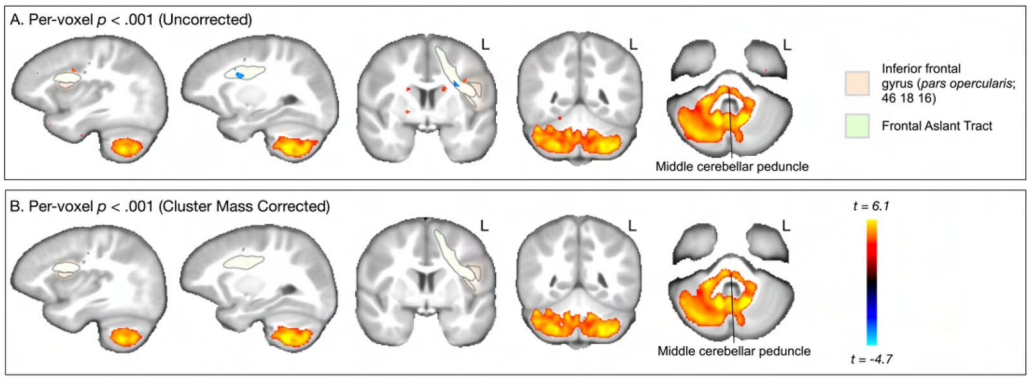

Figure 6. Whole brain, voxel-wise analysis of the interaction effect showing how age moderates the association between SRT performance and RNT (model Equation 3). (A) Uncorrected ($p < 0.001$) clusters are highlighted for regions and pathways reviewed in the Introduction. Areas in red spectrum indicate a positive interaction slope, and blue indicates a negative interaction slope. (B) Cluster mass corrected ($p < 0.001$) results show only clusters in cerebellar gray and white matter.

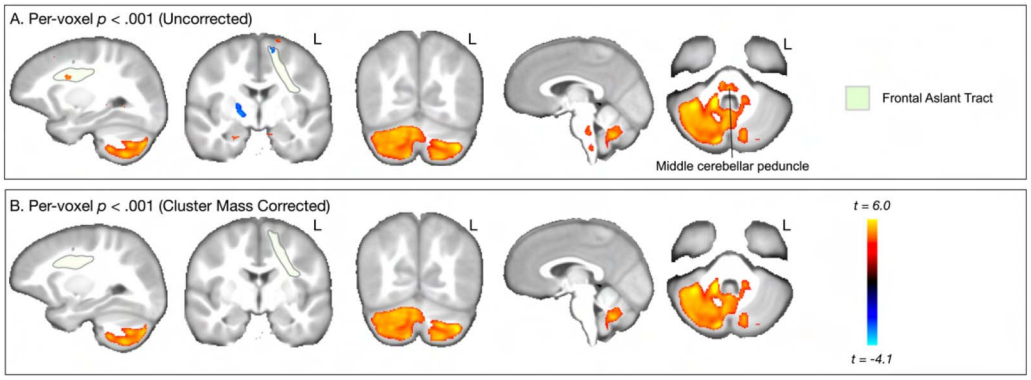

Figure 7. Whole brain, voxel-wise analysis of the interaction effect showing how age moderates the association between SRT performance and HNT (model Equation 4). (A) Uncorrected ($p < 0.001$) clusters are highlighted for regions and pathways reviewed in the Introduction. Areas in red spectrum indicate a positive interaction slope, and blue indicates a negative interaction slope. (B) Cluster mass corrected ($p < 0.001$) results show only clusters in cerebellar gray and white matter.

Our primary aim for this analysis was to examine the association between SRT performance and diffusion properties. Since there are 100 nodes along the tract profile, rather than conducting separate tests for each node, we examined each tract in a series of GAMs. We were mainly interested in whether SRT performance was moderated by placement (NodeID) along the tract profile. That is, we sought to examine whether performance differences were evident at certain points along the tract, but not others. This is the interaction effect.

Unlike traditional linear models, GAMs do not return a single, unified statistic summarizing the interaction. Instead, the interaction can be assessed through changes in the model fit (e.g., via

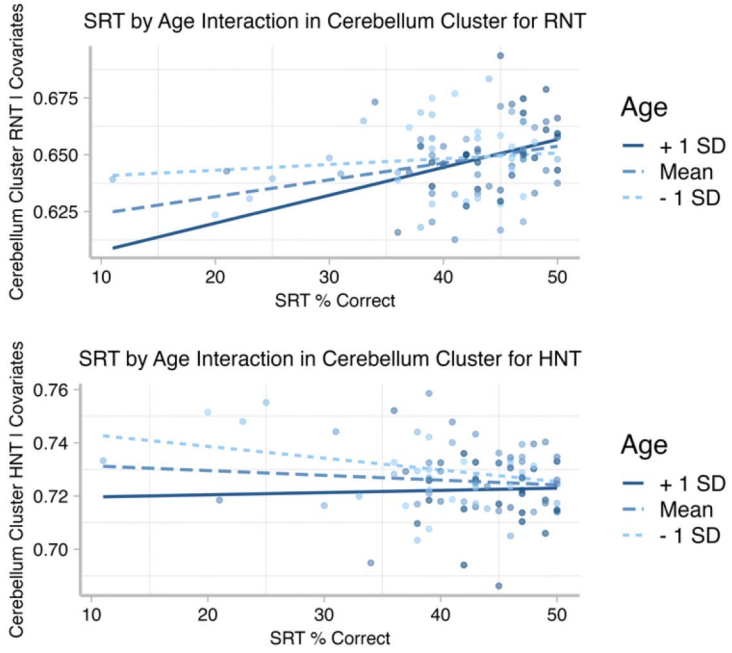

Figure 8. Residualized scatterplots show that age moderates the association between (top) SRT performance and RNT (restricted diffusion); and (bottom) SRT performance and HNT (hindered diffusion) in the cerebellum. Data are recovered from the cluster-corrected voxels for the whole brain interaction analysis, for each participant.

deviance explained or likelihood ratio tests) and visually interpreted through plots of the fitted curves. Statistical significance can also be evaluated at specific points (knots) along the trajectory.

For each tract, we modeled a main effect of SRT predicting diffusion, and a second model in which the interaction of SRT and NodeID was tested. Using analysis of variance, we tested whether including the interaction explained significantly more variance (deviance) than the model with only the main effect of SRT. Table 2 shows that for all tracts, including the interaction term explains significantly more variance (all F tests comparing the two models were significant at $p < 0.001$). This means that associations between SRT and diffusion properties differed in magnitude depending on placement along the tract profile. Significance tests for age and ADHD symptomatology covariates are included in Supplemental Table S1, avalable at https://doi.org/10.1162/nol_a_00168. In line with previous findings by Palmer and colleagues (2022), age was negatively associated with HNT and positively associated with RNT for almost all tracts. Since the RSI model is a multicompartment model, it is logical that as RNT increased, HNT would similarly decrease. A more nuanced pattern was noted for ADHD symptomatology.

Specifically, ADHD symptomatology was associated with RNT and HNT, but the pattern of association varied by the tract under consideration. This is a potentially important avenue of investigation in future studies focused on ADHD. Despite the robust effects of age and ADHD symptomatology, the interaction effects we reported for the SRT held.

With these interaction effects established, we conducted difference tests (essentially independent samples t tests) at each node, assessing high versus low performers (defined by the median split). Because this amounts to 100 tests for each tract, we corrected for multiple comparisons using the false discovery rate (FDR; Benjamini & Hochberg, 1995) procedure. These tract profiles are shown in Figures 9–12: Figure 9 and Figure 11 (for cortical association pathways) and Figure 10 and Figure 12 (for cerebellar pathways). In the figures, blue marks Node

Table 2. Model fit indices and comparisons for each tract profile

Tract	F (p value)	Main Effect AIC	% Deviance Explained (ME)	Interaction AIC	% Deviance Explained (Int)
Left FAT	9.1***	−33293.9	84.4	−33815.3	85.4
Right FAT	8.8***	−34275.3	85.9	−34756.8	86.7
Left AF	6.8***	−17568.4	43.7	−17878.1	46.4
Right AF	9.2***	−16672.4	31.2	−17138.4	35.2
Left SLF III	8.7***	−31870.7	70.8	−32314.8	72.5
Right SLF III	7.9***	−30573.8	68.7	−30937.1	70.2
Left SCP	9.7***	−3850.8	13.7	−4296.7	21.2
Right SCP	8.91***	−6406.8	14.0	−6827.3	20.8
Left MCP	7.07***	−7257.1	25.7	−7539.2	28.3
Right MCP	7.37***	−7516.1	28.8	−7821.1	31.5
Left ICP	12.4***	−27445.7	53.2	−28132.1	57.0
Right ICP	16.8***	−14909.4	24.6	−15979.6	33.3

Note. AIC = Akaike information criterion; ME = main effect; Int = interaction effect; FAT = frontal aslant tract; AF = arcuate fasciculus; SLF III = superior longitudinal fasciculus III; SCP, MCP, ICP = superior, middle, and inferior cerebellar peduncles.

*** $p < 0.001$.

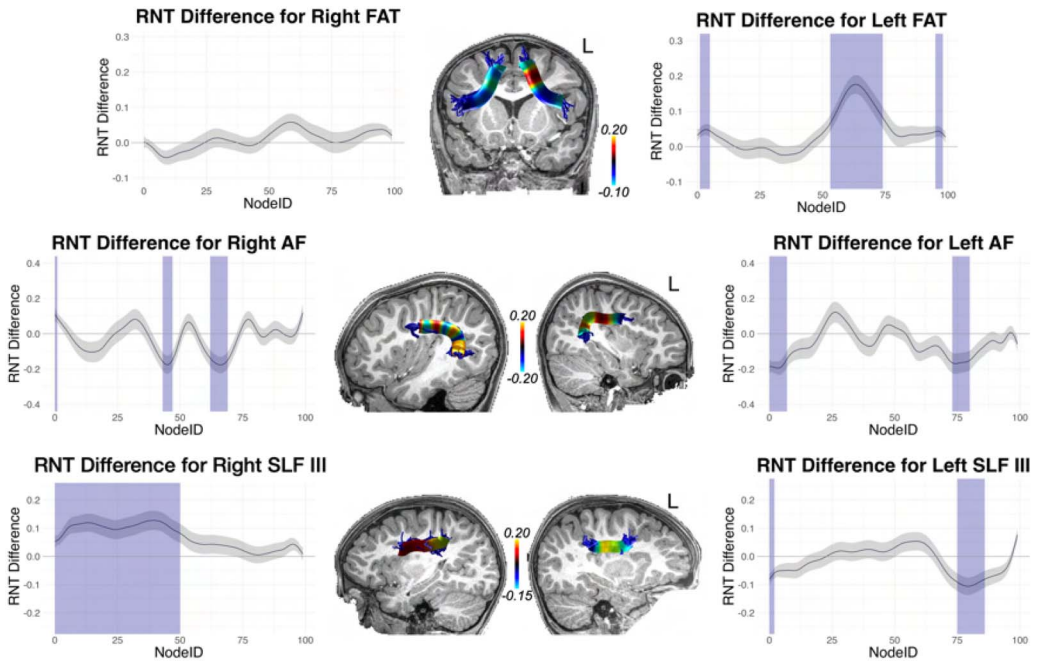

Figure 9. High vs. low SRT performance differences across tract profiles for frontal aslant tract (FAT), arcuate fasciculus (AF), and superior longitudinal fasciculus III (SLF III), for the RNT metric. The *y* axis reports the difference score for high vs. low performers determined by median split. The *x* axis reports the node index for the 100 nodes along the tract profile. Blue indicates the difference was statistically significant after false discovery rate (FDR) correction. The difference scores from the statistical analysis are mapped to representative tracts overlaid on T1 images for each tract.

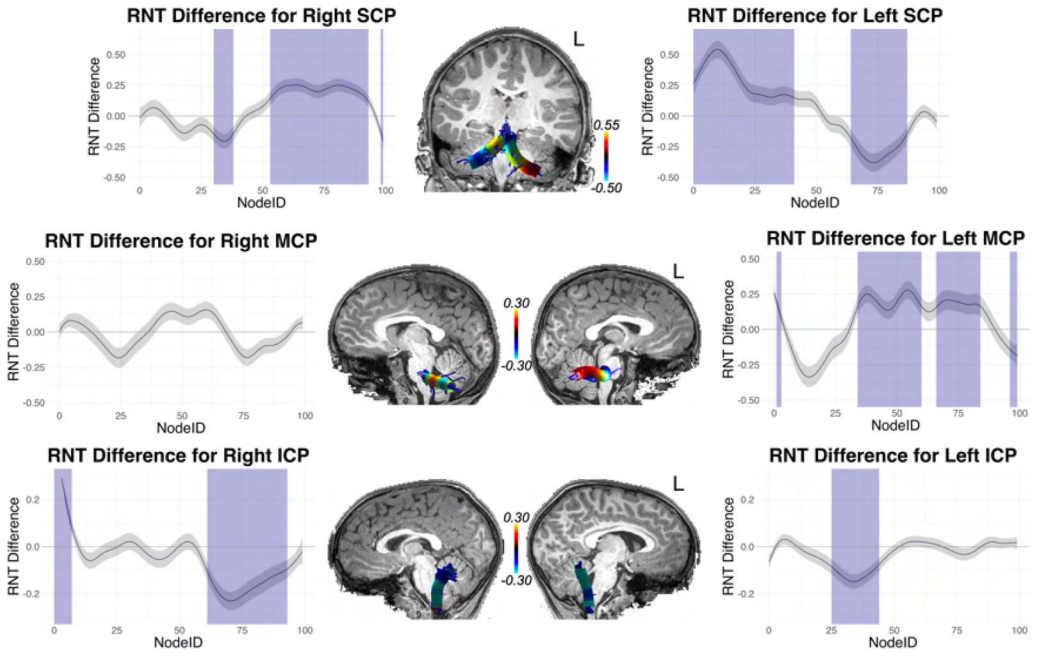

Figure 10. High vs. low SRT performance differences across tract profiles for superior (SCP), middle (MCP), and inferior (ICP) cerebellar peduncles, for the RNT metric. The *y* axis reports the difference score for high vs. low performers determined by median split. The *x* axis reports the node index for the 100 nodes along the tract profile. Blue indicates the difference was statistically significant after FDR correction. The difference scores from the statistical analysis are mapped to representative tracts overlaid on T1 images for each tract.

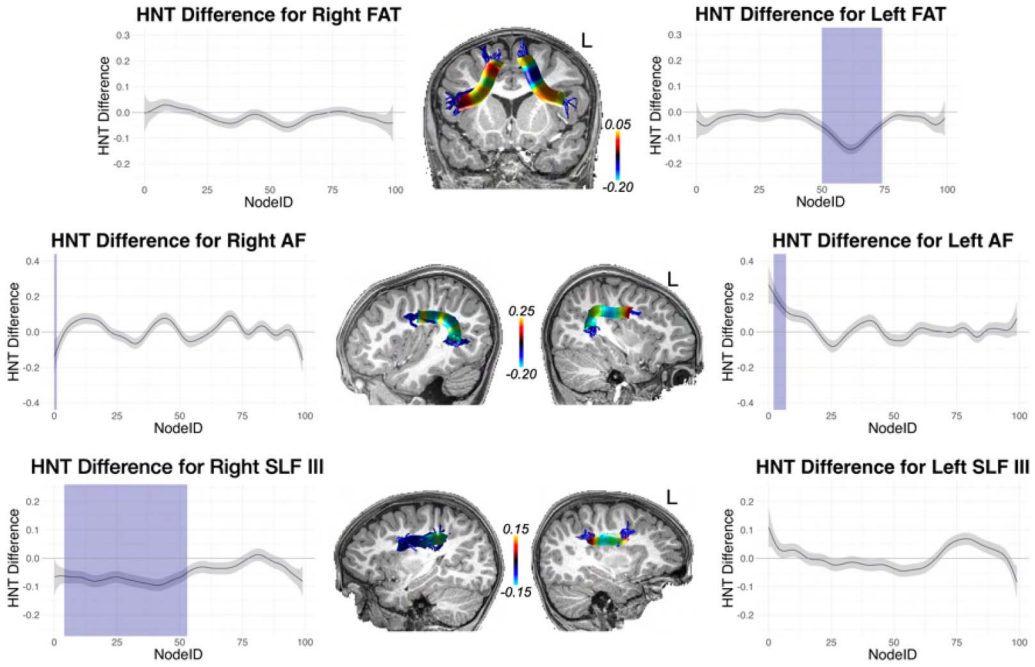

Figure 11. High vs. low SRT performance differences across tract profiles for FAT, AF, and SLF III, for the HNT metric. The *y* axis reports the difference score for high vs. low performers determined by median split. The *x* axis reports the node index for the 100 nodes along the tract profile. Blue indicates the difference was statistically significant after FDR correction. The difference scores from the statistical analysis are mapped to representative tracts overlaid on T1 images for each tract.

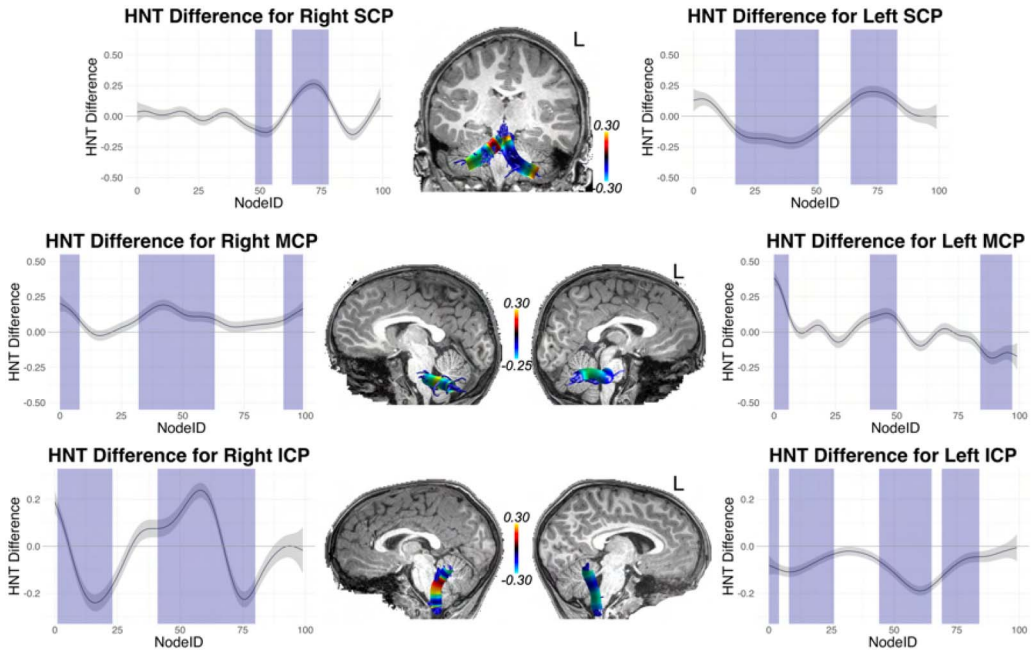

Figure 12. High vs. low SRT performance differences across tract profiles for SCP, MCP, and ICP, for the HNT metric. The *y* axis reports the difference score for high vs. low performers determined by median split. The *x* axis reports the node index for the 100 nodes along the tract profile. Blue indicates the difference was statistically significant after FDR correction. The difference scores from the statistical analysis are mapped to representative tracts overlaid on T1 images for each tract.

IDs that survived the FDR correction. In general, the results were similar for RNT and HNT, just in opposite directions.

As Figures 9–12 show, for FAT significant nodes were identified along the tract and highlighted in blue. No significant nodes were identified for the right FAT.

Although no significant clusters were identified in AF and SLF III in the whole brain analysis, fiber tract segmentation revealed significant RNT differences between above and below median SRT performance groups at considerable intervals along the tract profiles for SLF III, especially on the right hemisphere. In fact, no differences were found in left SLF III for the HNT metric. There were also significant differences in SRT performance for the left and right AF tract profiles, but these were not extensive, and were at isolated points along the tract.

We also examined significant differences in RNT between SRT performance groups for the cerebellar peduncles. The left and right SCP and ICP both contained large intervals with significant differences at those nodes. For MCP, differences were found only on the left for RNT, but bilaterally for HNT.

DISCUSSION

Updated models of speech neurobiology implicate a network of gray matter regions and the white matter pathways that connect them in speech production. Despite progress in identifying these regions and pathways, there are many questions that remain about how this speech network develops in early childhood. We examined this development in 4–7 year olds (half of whom were diagnosed with ADHD) who varied considerably in speech ability as measured by a speech task, the SRT. Our results revealed several key findings: (1) performance on the SRT is associated with differences in gray matter cellularity in regions identified as critical for speech production; (2) performance on the SRT further predicts differences in diffusion metrics along white matter tracts related to speech production; and (3) the association between speech task performance and gray and white matter cellularity changes as a function of age. These findings must be understood in the context of limitations in the current study, which include the mixed sample of ADHD and typically developing children, the specific measurement of speech using the SRT, and the measurement of cellularity and white matter properties using the RSI model. These limitations are discussed in detail below. Despite these limitations, the findings offer more specific details about how speech networks are organized during early childhood and, especially, provide insights about cortical and cerebellar regions and pathways that support these emerging networks.

Performance on the SRT Is Associated With Cellularity Differences in Frontal Brain Regions and Pathways Associated With Speech

In the whole brain analysis, we observed that (1) higher RNT in left and right pars opercularis was associated with better performance on the SRT, and (2) reduced RNT and increased HNT in the right pre-SMA/SMA were similarly linked to better SRT performance. However, neither finding survived multiple comparison correction. While these regions align with prior literature, these results should be interpreted cautiously. We provide a brief discussion of these findings with this limitation in mind, starting with the pars opercularis before addressing the pre-SMA/SMA.

The left pars opercularis has been implicated in speech neurobiology models. For instance, in the context of the GODIVA model (Guenther, 2016), this region may house cell populations representing syllable motor programs independent of semantic content (Ghosh et al., 2008).

Similarly, Hickok's model (Hickok et al., 2023) posits that the pars opercularis is involved in syllable sequencing. While our findings align with these models, the bilateral association observed in our data may reflect developmental factors, and previous research suggests that lateralization of language function increases with age. For example, Holland et al. (2001) showed that left lateralization in the inferior frontal cortex strengthens from ages 7 to 18 during a verb generation task. Similarly, Olulade et al. (2020) found that younger children (aged 4–8) show stronger activation in homologues of the right hemisphere during fMRI language tasks, with this pattern decreasing through adolescence. Our bilateral findings in pars opercularis may therefore reflect the substantial contribution of the right hemisphere to speech in younger children.

Furthermore, age moderated the association between SRT performance and RNT in the left pars opercularis, with stronger associations observed in older children, consistent with increased left lateralization over development.

The relationship between restricted diffusion and performance remains speculative, but can be informed by prior histologic studies. Palmer et al. (Palmer et al., 2022) suggested that age-related increases in restricted diffusion in gray matter could reflect changes such as increased myelination, neurite density, dendritic sprouting, or cell body growth (neuronal or glial). White and colleagues (White, Leergaard, et al., 2013; White, McDonald, et al., 2013; White et al., 2014), in developing the RSI model, highlighted its sensitivity to these microstructural properties. Based on this, we suggest that the observed associations may reflect these underlying tissue changes. However, given that these findings did not survive the cluster correction, they should be interpreted with appropriate caution and considered preliminary.

In the white matter of FAT, we can speculate that these associations have more to do with myelination of the pathway, which reduces the volume of extracellular space and also reduces the permeability of axonal membranes. This would lead to an increase in the signal in the restricted compartment. The AFQ analysis of the FAT showed that this effect was predominantly unilateral. In fact, no performance differences in the right FAT were statistically significant after FDR correction. Thus, unlike the finding in pars opercularis gray matter, the finding in FAT was prominently left lateralized. Moderating effects of age were also left lateralized. It is possible that for FAT white matter, connecting inferior frontal gyrus and pre-SMA/SMA cortical regions, the left FAT is more critical for speech than the right FAT (Dick et al., 2019). This is supported by studies in adults, which have shown that left FAT integrity is associated with stuttering (Kemerdere et al., 2016; Kronfeld-Duenias et al., 2016; Misaghi et al., 2018), speech arrest during tumor resection and intraopertive electrostimulation (Fujii et al., 2015; Vassal et al., 2014), post-stroke aphasia (Basilakos et al., 2014), and speech apraxia (Zhong et al., 2022). In this latter study, damage to the white matter and not the gray matter was the best predictor of speech impairment, suggesting that disconnection of the connectivity is a stronger factor for predicting motor speech deficits. Our findings are consistent with this possibility.

We also identified a small cluster in the right pre-SMA/SMA showing an association between SRT performance and reduced RNT/increased HNT. However, this cluster was small and did not survive cluster correction, so these findings should be interpreted with caution. The involvement of this region is consistent with previous evidence on the role of pre-SMA/SMA bilaterally in speech production (Alario et al., 2006; Bohland & Guenther, 2006; Tremblay & Gracco, 2009, 2010). For example, stimulation of pre-SMA/SMA during awake surgery can cause speech arrest (Lu et al., 2021), and Bohland and Guenther (2006) showed that even simple syllable sequences engage the pre-SMA/SMA bilaterally as part of the basic speech production network.

The direction of the effect—less restricted diffusion (and more hindered diffusion) being associated with better performance—differs from our other findings, making interpretation more challenging. Changes in diffusion properties can reflect various microstructural processes, such as increased dendritic pruning, which might enhance the processing efficiency of neural assemblies in the pre-SMA/SMA and result in reduced restricted diffusion and increased hindered diffusion signals. While this is a plausible explanation, it remains speculative and would require histological validation.

Performance on the SRT Is Associated With Cellularity Differences in Cerebellar White and Gray Matter

The whole brain analysis revealed that (1) higher RNT and HNT in left and right Crus I and II was associated with better SRT performance; and (2) higher RNT and HNT was associated with cerebellar white matter pathways: the SCP (for RNT only), MCP, and ICP. While for RNT, findings from cerebellar gray matter and MCP/ICP survived cluster correction, the SCP clusters did not (no clusters survived for HNT). Thus, associations with SCP should be interpreted with this caveat in mind.

The role of the cerebellum in speech motor control has long been attributed to the organization and coordination of motor commands necessary for speech production, but is particularly important for rapid speech (Ackermann, 2008; Guenther, 2016) or for more complex syllable sequences (Bohland & Guenther, 2006). The developmental importance of finely timed speech has been demonstrated in studies of children with early speech deficits, which found that poorer speech outcomes were associated with right cerebellar tumors (Morgan et al., 2011). This is consistent with adult cerebellar lesion studies (Urban et al., 2003), and the established connectivity of inferior frontal regions with the contralateral right cerebellum (Morgan et al., 2011). Results from the present study indicated left and right findings in the gray matter of the cerebellum, especially in the Crus I and Crus II cerebellar lobules. However, fMRI activation during speech and foci collected from meta-analyses of word and sentence reading have highlighted bilateral associations between speech and cerebellar gray matter (Brown et al., 2005; Guenther, 2016; Turkeltaub et al., 2002). Further, bilateral activation of Crus I and Crus II has been reported during speech production tasks and during silent syllable repetition tasks conducted in the MRI magnet (Bohland & Guenther, 2006; Correia et al., 2020; Geva et al., 2021; Ghosh et al., 2008; Liégeois et al., 2016; Peeva et al., 2010; Shuster & Lemieux, 2005). Thus, our findings are in line with previous literature that suggests motor control of speech is not limited to the right cerebellum.

The connectivity of the cerebellum with cortical and subcortical structures in the cerebral cortex is established through the cerebellar peduncles, white matter tracts that have been shown to play a role in aspects of speech fluency and motor speech production (Guenther, 2016; Johnson et al., 2022; Jossinger et al., 2024). Jossinger and colleagues investigated the role of the cerebellar peduncles in different components of speech processing, and found that verbal fluency was associated with the right SCP, whereas speaking rate was associated with the right MCP (Jossinger et al., 2024). A similar pattern is observed in children who stutter, as early developmental differences have been demonstrated in the right ICP between children who stutter and their age-matched peers (Johnson et al., 2022). However, the association between the cerebellar peduncles and motor speech production is not restricted to the right cerebellar peduncles. In adults who stutter, speech rate has been associated with white matter cellular properties in the left ICP (Jossinger et al., 2021). In addition, reduced integrity of the white matter has been observed for all three cerebellar peduncles in adolescents and adults who stutter (Connally et al., 2014), confirming the notion that motor speech production is

necessarily lateralized right. Our bilateral findings in the SCP, MCP, and ICP support the idea that key aspects of speech production may be organized bilaterally within the white matter pathways that connect the cerebellum to the cerebral cortex. The findings in the SCP from the whole brain analysis did not survive cluster correction, but our analysis of the SCP tract profiles revealed several significant nodes, which suggests that there may be some relationship between white matter cellular properties and speech performance that requires additional study to tease apart. Although both the left and right ICPs showed significant nodes, only the left MCP demonstrated a difference in SRT performance between nodes. We may have observed these differences because the cerebellar peduncles play different roles in motor speech processing, as noted by Jossinger et al. (2024), but understanding this relationship requires further analysis of different speech properties.

The findings from the present study demonstrate that greater differences in performance on a speech production task are associated with higher RNT and HNT in gray matter of the cerebellum, and higher RNT and lower HNT in white matter of the cerebellar peduncles (based on the tract profile analysis). Based on our knowledge of how RSI modulates developmental and maturational processes, we can speculate on the nature of the association, but we are unable to make definitive claims about the relationship between the restricted diffusion signal and speech performance without using more direct measurements. Developmental processes such as dendritic sprouting, myelination, and increasing neurite diameter result in a decrease in extracellular space, which in turn causes the signal to increase within the cellular compartment (Palmer et al., 2022). In particular, higher myelination is associated with greater speed of conductance for information traveling between neurons (Jossinger et al., 2021; Palmer et al., 2022; Zhong et al., 2022). We may tentatively conclude that an increase in RNT and decrease in HNT, possibly driven by developmental processes such as myelination, could lead to faster conduction of information and thus better performance on a speech task. This would be in line with the results from our whole brain analysis, which suggested that higher restricted diffusion signal was positively associated with speech performance, and that age moderated the strength of this association, which increased with age. While these conclusions are speculative, understanding the relationship between microstructural properties of gray and white matter and speech performance allows us to establish a relationship that may be further investigated in the future.

Tract Profile Analysis Reveals More Detailed Relationship Between SRT Performance and Dorsal Stream Fiber Pathways

Although the whole brain analysis did not reveal significant associations between SRT performance and the AF or SLF III, the AFQ analysis identified significant differences in RNT between the above median and below median SRT groups, albeit with minimal differences for the AF. Both the AF and SLF III are known to connect regions critical for motor speech function, such as the IFG with STS/STG, and SMG (Bernal & Ardila, 2009; Duffau et al., 2003; Hickok & Poeppel, 2004, 2007), and AF connectivity is implicated in specific language impairment in children (Vydrova et al., 2015). These findings, though subtle, may provide converging evidence for the role of these tracts in motor speech function.

It is also important to interpret these results in the context of the model. GAMs are highly sensitive to small differences, and the whole brain analysis did not reveal associations between RNT and SRT performance in the AF or SLF III. However, tractography at the individual participant level leverages the native MRI space of each individual, whereas whole brain analyses rely on registration to a template space, which can reduce spatial specificity

and sensitivity for structures of interest. Traditional fiber tracking methods, which average diffusion metrics across an entire fiber bundle, may miss localized relationships within the tract. Diffusion metrics can vary significantly along the trajectory of a tract (Yeatman et al., 2011). By creating tract profiles that examine diffusion metrics at specific nodes along the tract, methods like AFQ can reveal relationships that might otherwise remain obscured. Investigating white matter tracts with such approaches is therefore a crucial step toward a more nuanced understanding of the relationship between white matter microstructural properties and diffusion metrics.

Our results underscore the potential value of the AFQ findings in advancing our understanding of the neural speech network. This is especially the case for right SLF III, which showed a sustained difference across the profile of a large part of the anterior tract. It was also evident for left SLF III in the posterior part of the tract in the white matter near the SMG. This is consistent with Duffau's work showing the importance of this white matter for processing phonological information during speech production (Duffau et al., 2003). In that study, electrostimulation during awake surgery of white matter connecting SMG and IFG disrupted speech production. Our results showing such an association in a sample of very young children is novel and provides additional support for the importance of this pathway to speech production.

Associations With Basal Ganglia Gray Matter and Corticobulbar White Matter

In clinical samples with developmental speech and language disorders, researchers have focused on the structure of the basal ganglia and the corticobulbar tract (Liégeois et al., 2013; Morgan et al., 2018; Northam et al., 2019). For example, Morgan and colleagues (2018) examined 41 adolescents with developmental speech or language disorders alongside 45 typical controls using DWI. Their results indicated that developmental speech disorder was associated with reduced fractional anisotropy in the left corticobulbar tract (see also Liégeois et al., 2013). Given that the corticobulbar tract follows a well-defined path through the internal capsule's white matter and the cerebral peduncle (Dick et al., 2014), it is amenable to voxel-wise analyses linking its structure to SRT performance. Nonetheless, our whole brain analysis did not reveal any behavioral associations with this white matter tract. It is possible that alternative tasks (Pigdon, Willmott, Reilly, Conti-Ramsden, Liegeois, et al., 2020) or studies involving clinical populations with speech disorder, dysarthria, or dyspraxia (Liégeois et al., 2013; Morgan et al., 2018; Northam et al., 2019) might uncover such links, but we did not find it in the present study.

With respect to the basal ganglia, we observed an age-related interaction between SRT performance and the left and right caudate nucleus (see Figure 6), although this finding did not survive cluster correction. This outcome aligns with previous studies that underscore the significance of basal ganglia structures in clinical contexts (Belton et al., 2003; Rowan et al., 2007). For instance, abnormalities in the basal ganglia have been noted in individuals with FOXP2 mutations (Belton et al., 2003), and children with focal basal ganglia strokes often exhibit language impairments (Rowan et al., 2007). One limitation of the voxel-wise approach is that small clusters, which might be functionally meaningful, may not reach significance after correction for multiple comparisons. However, the age-by-SRT performance interaction was overwhelmingly represented in the cerebellum, which could instead simply suggest the prominent importance of the contributions of the cerebellum to speech development. This too could benefit from further investigation in clinical samples using the methods applied here.

Limitations

One limitation of the current study regards the sample makeup, which included both children who are typically developing and children with ADHD, and contained a higher percentage of boys than girls. Children who are atypically developing, such as those with ADHD, are at risk for developing comorbid psychiatric and speech disorders (Booster et al., 2012), and a mixed sample over-represented by boys may not be generalizable to a broader population. However, few studies focusing on neural speech networks in early childhood exist, and the findings from this study provide critical background for understanding the implementation of speech production in the brain at early stages of speech development. We did not find performance differences on the SRT, and we further controlled for ADHD symptomatology. This suggests that treating the ADHD and typically developing children as a representative sample for performance on this task is justified.

A second limitation concerns the speech task implemented in the current research, the SRT. For this study, we focused on a single speech task that measured the repetition of multisyllabic utterances. Although the SRT measures expressive speech production (Shriberg et al., 2009), it is not sensitive to the different phases of speech that may occur during repetition. For example, the SRT is unable to distinguish between prearticulatory encoding and the actual transformation of phonological planning into motor execution of speech. The SRT is a speech task that measures the repetition of single, multisyllabic nonwords and thus cannot provide insight into how connected speech may play a role in speech processing. Research has shown that many factors may be involved with nonword repetition, such as phonological memory, oromotor sequencing ability, word reading, and oromotor control (Pigdon, Willmott, Reilly, Conti-Ramsden, & Morgan, 2020). Despite these limitations, the SRT is a child-friendly phonemic task that has been validated as an assessment of motor planning difficulties (Rvachew & Matthews, 2017), and may be considered as part of a battery of speech and language tasks in the future to provide a more complete picture of speech development.

Finally, we must carefully consider what our diffusion metrics of interest actually measure. Although we can provide speculation for what cellular processes are modulated by restricted and hindered diffusion, we cannot definitively identify the developmental and maturational processes underlying differences in diffusion metrics. The issue of specificity is a problem for diffusion measures more broadly, not just RSI. In fact, a major strength of RSI beyond traditional diffusion measures, such as DTI, is that we are able to observe differences in cellularity in both gray and white matter. While RSI has its constraints, much like other DWI reconstruction methods, it provides a more complete picture of neural development across gray matter ROIs and white matter pathways.

Conclusion

Characterizing the structural development of the neural speech network in early childhood is important for understanding speech acquisition. In this investigation, we found that (1) performance on the SRT is associated with differences in gray matter cellularity in regions identified as critical for speech production, including IFG and several cortical regions which did not survive cluster correction; (2) performance on the SRT further predicts differences in diffusion metrics along white matter tracts related to speech production, especially left FAT, left and right SLF III, and the cerebellar peduncles; and (3) the association between speech task performance and gray and white matter cellularity changes as a function of age in these regions and pathways. The findings suggest that individual differences in speech performance are reflected in structural gray and white matter differences as measured by restricted and hindered diffusion properties, and offer important insights into how the neural speech network develops in children during early childhood.

ACKNOWLEDGMENTS

We thank the parents and children who participated in the AHEAD study from which these data were analyzed. We also thank Anders Dale and Donald Hagler for help with RSI reconstruction, and M. Okan Irfanoglu and Carlo Pierpaoli for recommended DWI reconstruction steps for ABCD diffusion acquisition protocols, and improvements to those protocols.

FUNDING INFORMATION

Paulo Graziano, National Institute of Mental Health (https://dx.doi.org/10.13039/100000025), Award ID: R01MH112588. Paulo Graziano, National Institute of Diabetes and Digestive and Kidney Diseases (https://dx.doi.org/10.13039/100000062), Award ID: R01DK119814. Paulo Graziano, National Institute of Mental Health (https://dx.doi.org/10.13039/100000025), Award ID: R56MH108616. Anthony Steven Dick, National Institute of Mental Health (https://dx.doi.org/10.13039/100000025), Award ID: R01MH112588. Anthony Steven Dick, National Institute of Diabetes and Digestive and Kidney Diseases (https://dx.doi.org/10.13039/100000062), Award ID: R01DK119814. Anthony Steven Dick, National Institute of Mental Health (https://dx.doi.org/10.13039/100000025), Award ID: R56MH108616.

AUTHOR CONTRIBUTIONS

Marilyn Curtis: Formal analysis: Equal; Writing – original draft: Equal; Writing – review & editing: Equal. **Mohammadreza Bayat**: Data curation: Equal; Formal analysis: Equal; Writing – review & editing: Equal. **Dea Garic**: Conceptualization: Supporting; Data curation: Equal; Formal analysis: Equal; Writing – review & editing: Equal. **Alliete R. Alfano**: Formal analysis: Supporting; Supervision: Equal; Writing – review & editing: Supporting. **Melissa Hernandez**: Data curation: Equal. **Madeline Curzon**: Data curation: Equal. **Andrea Bejarano**: Data curation: Equal; Project administration: Supporting. **Pascale Tremblay**: Methodology: Equal; Writing – review & editing: Equal. **Shannon Marie Pruden**: Writing – review & editing: Supporting. **Paulo Graziano**: Conceptualization: Equal; Funding acquisition: Equal; Methodology: Equal; Supervision: Equal; Writing – review & editing: Equal. **Anthony Steven Dick**: Conceptualization: Lead; Data curation: Lead; Formal analysis: Lead; Funding acquisition: Equal; Investigation: Lead; Methodology: Lead; Project administration: Equal; Resources: Equal; Supervision: Lead; Writing – original draft: Lead; Writing – review & editing: Lead.

DATA AND CODE AVAILABILITY STATEMENT

Code for analyses are supplied at https://github.com/anthonystevendick/curtis_srt. Data are available at https://nda.nih.gov/edit_collection.html?id=2781.

REFERENCES

Ackermann, H. (2008). Cerebellar contributions to speech production and speech perception: Psycholinguistic and neurobiological perspectives. *Trends in Neurosciences*, *31*(6), 265–272. https://doi.org/10.1016/j.tins.2008.02.011, PubMed: 18471906

Alario, F.-X., Chainay, H., Lehericy, S., & Cohen, L. (2006). The role of the supplementary motor area (SMA) in word production. *Brain Research*, *1076*(1), 129–143. https://doi.org/10.1016/j.brainres.2005.11.104, PubMed: 16480694

[APA] American Psychiatric Association. (2013). *Diagnostic and statistical manual of mental disorders* (5th ed.). https://doi.org/10.1176/appi.books.9780890425596

Andersson, J. L., Graham, M. S., Drobnjak, I., Zhang, H., Filippini, N., & Bastiani, M. (2017). Towards a comprehensive framework for movement and distortion correction of diffusion MR images: Within volume movement. *NeuroImage*, *152*, 450–466. https://doi.org/10.1016/j.neuroimage.2017.02.085, PubMed: 28284799

Andersson, J. L., Graham, M. S., Zsoldos, E., & Sotiropoulos, S. N. (2016). Incorporating outlier detection and replacement into a non-parametric framework for movement and distortion correction of diffusion mr images. *NeuroImage*, *141*, 556–572. https://doi.org/10.1016/j.neuroimage.2016.06.058, PubMed: 27393418

Andersson, J. L., Skare, S., & Ashburner, J. (2003). How to correct susceptibility distortions in spin-echo echo-planar images: Application to diffusion tensor imaging. *NeuroImage*, *20*(2), 870–888. https://doi.org/10.1016/S1053-8119(03)00336-7, PubMed: 14568458

Argyropoulos, G. P., Watkins, K. E., Belton-Pagnamenta, E., Liégeois, F., Saleem, K. S., Mishkin, M., & Vargha-Khadem, F. (2019). Neocerebellar crus I abnormalities associated with a speech and language disorder due to a mutation in FOXP2. *Cerebellum*, *18*(3), 309–319. https://doi.org/10.1007/s12311-018-0989-3, PubMed: 30460543

Baker, L., & Cantwell, D. P. (1992). Attention deficit disorder and speech/language disorders. *Comprehensive Mental Health Care*, *2*(1), 3–16.

Bammer, R., Markl, M., Barnett, A., Acar, B., Alley, M., Pelc, N., Glover, G., & Moseley, M. (2003). Analysis and generalized correction of the effect of spatial gradient field distortions in diffusion-weighted imaging. *Magnetic Resonance in Medicine*, *50*(3), 560–569. https://doi.org/10.1002/mrm.10545, PubMed: 12939764

Barbeau, E. B., Descoteaux, M., & Petrides, M. (2020). Dissociating the white matter tracts connecting the temporo-parietal cortical region with frontal cortex using diffusion tractography. *Scientific Reports*, *10*(1), 8186. https://doi.org/10.1038/s41598-020-64124-y, PubMed: 32424290

Barnett, A. S., Hutchinson, E., Irfanoglu, M. O., & Pierpaoli, C. (2014). Higher order correction of eddy current distortion in diffusion weighted echo planar images. In *Joint Annual Meeting ISMRM-ESMRMB: Fashioning MR to improve global healthcare* (p. 5119). ISMRM.

Barnett, A. S., Irfanoglu, M. O., Landman, B., Rogers, B., & Pierpaoli, C. (2021). Mapping gradient nonlinearity and miscalibration using diffusion-weighted MR images of a uniform isotropic phantom. *Magnetic Resonance in Medicine*, *86*(6), 3259–3273. https://doi.org/10.1002/mrm.28890, PubMed: 34351007

Basilakos, A., Fillmore, P. T., Rorden, C., Guo, D., Bonilha, L., & Fridriksson, J. (2014). Regional white matter damage predicts speech fluency in chronic post-stroke aphasia. *Frontiers in Human Neuroscience*, *8*, Article 845. https://doi.org/10.3389/fnhum.2014.00845, PubMed: 25368572

Belton, E., Salmond, C. H., Watkins, K. E., Vargha-Khadem, F., & Gadian, D. G. (2003). Bilateral brain abnormalities associated with dominantly inherited verbal and orofacial dyspraxia. *Human Brain Mapping*, *18*(3), 194–200. https://doi.org/10.1002/hbm.10093, PubMed: 12599277

Benjamini, Y., & Hochberg, Y. (1995). Controlling the false discovery rate: A practical and powerful approach to multiple testing. *Journal of the Royal Statistical Society, Series B: Statistical Methodology*, *57*(1), 289–300. https://doi.org/10.1111/j.2517-6161.1995.tb02031.x

Bernal, B., & Altman, N. (2009). Neural networks of motor and cognitive inhibition are dissociated between brain hemispheres: An fMRI study. *International Journal of Neuroscience*, *119*(10), 1848–1880. https://doi.org/10.1080/00207450802333029, PubMed: 19922390

Bernal, B., & Ardila, A. (2009). The role of the arcuate fasciculus in conduction aphasia. *Brain*, *132*(9), 2309–2316. https://doi.org/10.1093/brain/awp206, PubMed: 19690094

Bernard, F., Zemmoura, I., Ter Minassian, A., Lemée, J.-M., & Menei, P. (2019). Anatomical variability of the arcuate fasciculus: A systematical review. *Surgical and Radiologic Anatomy*, *41*(8), 889–900. https://doi.org/10.1007/s00276-019-02244-5, PubMed: 31028450

Bihan, D. L. (1995). Molecular diffusion, tissue microdynamics and microstructure. *NMR in Biomedicine*, *8*(7), 375–386. https://doi.org/10.1002/nbm.1940080711, PubMed: 8739274

Blood, G. W., Ridenour, V. J., Qualls, C. D., & Hammer, C. S. (2003). Co-occurring disorders in children who stutter. *Journal of Communication Disorders*, *36*(6), 427–448. https://doi.org/10.1016/S0021-9924(03)00023-6, PubMed: 12967738

Bohland, J. W., & Guenther, F. H. (2006). An fMRI investigation of syllable sequence production. *NeuroImage*, *32*(2), 821–841. https://doi.org/10.1016/j.neuroimage.2006.04.173, PubMed: 16730195

Bombonato, C., Cipriano, E., Pecini, C., Casalini, C., Bosco, P., Podda, I., Tosetti, M., Biagi, L., & Chilosi, A. M. (2022). Relationship among connectivity of the frontal aslant tract, executive functions, and speech and language impairment in children with childhood apraxia of speech. *Brain Sciences*, *13*(1), Article 78. https://doi.org/10.3390/brainsci13010078, PubMed: 36672059

Booster, G. D., Dupaul, G. J., Eiraldi, R., & Power, T. J. (2012). Functional impairments in children with ADHD: Unique effects of age and comorbid status. *Journal of Attention Disorders*, *16*(3), 179–189. https://doi.org/10.1177/1087054710383239, PubMed: 20876886

Broce, I., Bernal, B., Altman, N., Tremblay, P., & Dick, A. S. (2015). Fiber tracking of the frontal aslant tract and subcomponents of the arcuate fasciculus in 5–8-year-olds: Relation to speech and language function. *Brain and Language*, *149*, 66–76. https://doi.org/10.1016/j.bandl.2015.06.006, PubMed: 26186231

Brown, S., Ingham, R. J., Ingham, J. C., Laird, A. R., & Fox, P. T. (2005). Stuttered and fluent speech production: An ALE meta-analysis of functional neuroimaging studies. *Human Brain Mapping*, *25*(1), 105–117. https://doi.org/10.1002/hbm.20140, PubMed: 15846815

Bruckert, L., Shpanskaya, K., McKenna, E. S., Borchers, L. R., Yablonski, M., Blecher, T., Ben-Shachar, M., Travis, K. E., Feldman, H. M., & Yeom, K. W. (2019). Age-dependent white matter characteristics of the cerebellar peduncles from infancy through adolescence. *Cerebellum*, *18*(3), 372–387. https://doi.org/10.1007/s12311-018-1003-9, PubMed: 30637673

Brunsing, R. L., Schenker-Ahmed, N. M., White, N. S., Parsons, J. K., Kane, C., Kuperman, J., Bartsch, H., Kader, A. K., Rakow-Penner, R., Seibert, T. M., Margolis, D., Rama, S. S., McDonald, C. R., Farid, N., Kesari, S., Hansel, D., Shabaik, A., Dale, A. M., & Karow, D. S. (2017). Restriction spectrum imaging: An evolving imaging biomarker in prostate MRI. *Journal of Magnetic Resonance Imaging*, *45*(2), 323–336. https://doi.org/10.1002/jmri.25419, PubMed: 27527500

Buchsbaum, B. R., Hickok, G., & Humphries, C. (2001). Role of left posterior superior temporal gyrus in phonological processing for speech perception and production. *Cognitive Science*, *25*(5), 663–678. https://doi.org/10.1207/s15516709cog2505_2

Catani, M., Mesulam, M. M., Jakobsen, E., Malik, F., Martersteck, A., Wieneke, C., Thompson, C. K., Thiebaut de Schotten, M., Dell'Acqua, F., Weintraub, S., & Rogalski, E. (2013). A novel frontal pathway underlies verbal fluency in primary progressive aphasia. *Brain*, *136*(8), 2619–2628. https://doi.org/10.1093/brain/awt163, PubMed: 23820597

Chang, D. C., Zhu, D. C., Choo, A. L., & Angstadt, M. (2015). White matter neuroanatomical differences in young children who stutter. *Brain*, *138*(3), 694–711. https://doi.org/10.1093/brain/awu400, PubMed: 25619509

Chang, H., & Fitzpatrick, J. M. (1992). A technique for accurate magnetic resonance imaging in the presence of field inhomogeneities. *IEEE Transactions on Medical Imaging*, *11*(3),

319–329. https://doi.org/10.1109/42.158935, PubMed: 18222873

Cohen, J. (1960). A coefficient of agreement for nominal scales. *Educational and Psychological Measurement*, *20*(1), 37–46. https://doi.org/10.1177/001316446002000104

Connally, E. L., Ward, D., Howell, P., & Watkins, K. E. (2014). Disrupted white matter in language and motor tracts in developmental stuttering. *Brain and Language*, *131*, 25–35. https://doi.org/10.1016/j.bandl.2013.05.013, PubMed: 23819900

Correia, J. M., Caballero-Gaudes, C., Guediche, S., & Carreiras, M. (2020). Phonatory and articulatory representations of speech production in cortical and subcortical fMRI responses. *Scientific Reports*, *10*(1), Article 4529. https://doi.org/10.1038/s41598-020-61435-y, PubMed: 32161310

Damico, J. S., Müller, N., & Ball, M. J. (Eds.). (2010). *The handbook of language and speech disorders*. Wiley. https://doi.org/10.1002/9781444318975

Destrieux, C., Fischl, B., Dale, A., & Halgren, E. (2010). Automatic parcellation of human cortical gyri and sulci using standard anatomical nomenclature. *NeuroImage*, *53*(1), 1–15. https://doi.org/10.1016/j.neuroimage.2010.06.010, PubMed: 20547229

Dick, A. S., Bernal, B., & Tremblay, P. (2014). The language connectome: New pathways, new concepts. *Neuroscientist*, *20*(5), 453–467. https://doi.org/10.1177/1073858413513502, PubMed: 24342910

Dick, A. S., Garic, D., Graziano, P., & Tremblay, P. (2019). The frontal aslant tract (FAT) and its role in speech, language and executive function. *Cortex*, *111*, 148–163. https://doi.org/10.1016/j.cortex.2018.10.015, PubMed: 30481666

Donaher, J., & Richels, C. (2012). Traits of attention deficit/hyperactivity disorder in school-age children who stutter. *Journal of Fluency Disorders*, *37*(4), 242–252. https://doi.org/10.1016/j.jfludis.2012.08.002, PubMed: 23218208

Druker, K., Hennessey, N., Mazzucchelli, T., & Beilby, J. (2019). Elevated attention deficit hyperactivity disorder symptoms in children who stutter. *Journal of Fluency Disorders*, *59*, 80–90. https://doi.org/10.1016/j.jfludis.2018.11.002, PubMed: 30477807

Duffau, H., Gatignol, P., Denvil, D., Lopes, M., & Capelle, L. (2003). The articulatory loop: Study of the subcortical connectivity by electrostimulation. *Neuroreport*, *14*(15), 2005–2008. https://doi.org/10.1097/00001756-200310270-00026, PubMed: 14561939

Fabiano, G. A., Pelham, W. E., Jr., Waschbusch, D. A., Gnagy, E. M., Lahey, B. B., Chronis, A. M., Onyango, A. N., Kipp, H., Lopez-Williams, A., & Burrows-MacLean, L. (2006). A practical measure of impairment: Psychometric properties of the impairment rating scale in samples of children with attention deficit hyperactivity disorder and two school-based samples. *Journal of Clinical Child and Adolescent Psychology*, *35*(3), 369–385. https://doi.org/10.1207/s15374424jccp3503_3, PubMed: 16836475

Frings, M., Dimitrova, A., Schorn, C. F., Elles, H.-G., Hein-Kropp, C., Gizewski, E. R., Diener, H. C., & Timmann, D. (2006). Cerebellar involvement in verb generation: An fMRI study. *Neuroscience Letters*, *409*(1), 19–23. https://doi.org/10.1016/j.neulet.2006.08.058, PubMed: 17046160

Fujii, M., Maesawa, S., Motomura, K., Futamura, M., Hayashi, Y., Koba, I., & Wakabayashi, T. (2015). Intraoperative subcortical mapping of a language-associated deep frontal tract connecting the superior frontal gyrus to Broca's area in the dominant hemisphere of patients with glioma. *Journal of Neurosurgery*, *122*(6), 1390–1396. https://doi.org/10.3171/2014.10.JNS14945, PubMed: 25816090

Geva, S., Schneider, L. M., Roberts, S., Khan, S., Gajardo-Vidal, A., Lorca-Puls, D. L., PLORAS Team, Hope, T. M. H., Green, D. W., & Price, C. J. (2021). Right cerebral motor areas that support accurate speech production following damage to cerebellar speech areas. *NeuroImage: Clinical*, *32*, Article 102820. https://doi.org/10.1016/j.nicl.2021.102820, PubMed: 34653836

Ghosh, S. S., Tourville, J. A., & Guenther, F. H. (2008). A neuroimaging study of premotor lateralization and cerebellar involvement in the production of phonemes and syllables. *Journal of Speech, Language, and Hearing Research*, *51*(5), 1183–1202. https://doi.org/10.1044/1092-4388(2008/07-0119), PubMed: 18664692

Glover, G., & Pelc, N. (1986). *Method for correcting image distortion due to gradient nonuniformity* [US Patent No. US-4591789-A]. US Patent and Trademark Office.

Graziano, P. A., Garic, D., & Dick, A. S. (2022). Individual differences in white matter of the uncinate fasciculus and inferior fronto-occipital fasciculus: Possible early biomarkers for callous-unemotional behaviors in young children with disruptive behavior problems. *Journal of Child Psychology and Psychiatry*, *63*(1), 19–33. https://doi.org/10.1111/jcpp.13444, PubMed: 34038983

Guenther, F. H. (2016). *Neural control of speech*. MIT Press. https://doi.org/10.7551/mitpress/10471.001.0001

Hagler, D. J., Jr., Ahmadi, M. E., Kuperman, J., Holland, D., McDonald, C. R., Halgren, E., & Dale, A. M. (2009). Automated white-matter tractography using a probabilistic diffusion tensor atlas: Application to temporal lobe epilepsy. *Human Brain Mapping*, *30*(5), 1535–1547. https://doi.org/10.1002/hbm.20619, PubMed: 18671230

Hagler, D. J., Jr., Hatton, S. N., Cornejo, M. D., Makowski, C., Fair, D. A., Dick, A. S., Sutherland, M. T., Casey, B. J., Barch, D. M., Harms, M. P., Watts, R., Bjork, J. M., Garavan, H. P., Hilmer, L., Pung, C. J., Sicat, C. S., Kuperman, J., Bartsch, H., Xue, F., … Dale, A. M. (2019). Image processing and analysis methods for the Adolescent Brain Cognitive Development Study. *NeuroImage*, *202*, Article 116091. https://doi.org/10.1016/j.neuroimage.2019.116091, PubMed: 31415884

Healey, E. C., & Reid, R. (2003). ADHD and stuttering: A tutorial. *Journal of Fluency Disorders*, *28*(2), 79–93. https://doi.org/10.1016/S0094-730X(03)00021-4, PubMed: 12809746

Hertrich, I., Dietrich, S., & Ackermann, H. (2016). The role of the supplementary motor area for speech and language processing. *Neuroscience and Biobehavioral Reviews*, *68*, 602–610. https://doi.org/10.1016/j.neubiorev.2016.06.030, PubMed: 27343998

Hickok, G., Buchsbaum, B., Humphries, C., & Muftuler, T. (2003). Auditory–motor interaction revealed by fMRI: Speech, music, and working memory in area Spt. *Journal of Cognitive Neuroscience*, *15*(5), 673–682. https://doi.org/10.1162/jocn.2003.15.5.673, PubMed: 12965041

Hickok, G., & Poeppel, D. (2000). Towards a functional neuroanatomy of speech perception. *Trends in Cognitive Sciences*, *4*(4), 131–138. https://doi.org/10.1016/S1364-6613(00)01463-7, PubMed: 10740277

Hickok, G., & Poeppel, D. (2004). Dorsal and ventral streams: A framework for understanding aspects of the functional anatomy of language. *Cognition*, *92*(1–2), 67–99. https://doi.org/10.1016/j.cognition.2003.10.011, PubMed: 15037127

Hickok, G., & Poeppel, D. (2007). The cortical organization of speech processing. *Nature Reviews Neuroscience*, *8*(5), 393–402. https://doi.org/10.1038/nrn2113, PubMed: 17431404

Hickok, G., Venezia, J., & Teghipco, A. (2023). Beyond Broca: Neural architecture and evolution of a dual motor speech coordination system. *Brain*, *146*(5), 1775–1790. https://doi.org/10.1093/brain/awac454, PubMed: 36746488

Holland, D., Kuperman, J. M., & Dale, A. M. (2010). Efficient correction of inhomogeneous static magnetic field-induced distortion in Echo Planar Imaging. *NeuroImage*, *50*(1), 175–183. https://doi.org/10.1016/j.neuroimage.2009.11.044, PubMed: 19944768

Holland, S. K., Plante, E., Byars, A. W., Strawsburg, R. H., Schmithorst, V. J., & Ball, W. S., Jr. (2001). Normal fMRI brain activation patterns in children performing a verb generation task. *NeuroImage*, *14*(4), 837–843. https://doi.org/10.1006/nimg.2001.0875, PubMed: 11554802

Irfanoglu, M. O., Modi, P., Nayak, A., Hutchinson, E. B., Sarlls, J., & Pierpaoli, C. (2015). *DR-BUDDI* (Diffeomorphic Registration for Blip-Up Blip-Down Diffusion Imaging) method for correcting echo planar imaging distortions. *NeuroImage*, *106*, 284–299. https://doi.org/10.1016/j.neuroimage.2014.11.042, PubMed: 25433212

Jobson, K. R., Hoffman, L. J., Metoki, A., Popal, H., Dick, A. S., Reilly, J., & Olson, I. R. (2024). Language and the cerebellum: Structural connectivity to the eloquent brain. *Neurobiology of Language*, *5*(3), 652–675. https://doi.org/10.1162/nol_a_00085, PubMed: 39175788

Johnson, C. A., Liu, Y., Waller, N., & Chang, S.-E. (2022). Tract profiles of the cerebellar peduncles in children who stutter. *Brain Structure and Function*, *227*(5), 1773–1787. https://doi.org/10.1007/s00429-022-02471-4, PubMed: 35220486

Jossinger, S., Kronfeld-Duenias, V., Zislis, A., Amir, O., & Ben-Shachar, M. (2021). Speech rate association with cerebellar white-matter diffusivity in adults with persistent developmental stuttering. *Brain Structure and Function*, *226*(3), 801–816. https://doi.org/10.1007/s00429-020-02210-7, PubMed: 33538875

Jossinger, S., Yablonski, M., Amir, O., & Ben-Shachar, M. (2024). The contributions of the cerebellar peduncles and the frontal aslant tract in mediating speech fluency. *Neurobiology of Language*, *5*(3), 676–700. https://doi.org/10.1162/nol_a_00098, PubMed: 39175785

Kemerdere, R., de Champfleur, N. M., Deverdun, J., Cochereau, J., Moritz-Gasser, S., Herbet, G., & Duffau, H. (2016). Role of the left frontal aslant tract in stuttering: A brain stimulation and tractographic study. *Journal of Neurology*, *263*(1), 157–167. https://doi.org/10.1007/s00415-015-7949-3, PubMed: 26559819

Kinoshita, M., de Champfleur, N. M., Deverdun, J., Moritz-Gasser, S., Herbet, G., & Duffau, H. (2015). Role of fronto-striatal tract and frontal aslant tract in movement and speech: An axonal mapping study. *Brain Structure and Function*, *220*(6), 3399–3412. https://doi.org/10.1007/s00429-014-0863-0, PubMed: 25086832

Kronfeld-Duenias, V., Amir, O., Ezrati-Vinacour, R., Civier, O., & Ben-Shachar, M. (2016). The frontal aslant tract underlies speech fluency in persistent developmental stuttering. *Brain Structure and Function*, *221*(1), 365–381. https://doi.org/10.1007/s00429-014-0912-8, PubMed: 25344925

Kruper, J., Yeatman, J. D., Richie-Halford, A., Bloom, D., Grotheer, M., Caffarra, S., Kiar, G., Karipidis, I. I., Roy, E., Chandio, B. Q., Garyfallidis, E., & Rokem, A. (2021). Evaluating the reliability of human brain white matter tractometry. *Aperture Neuro*, *1*(1), 1–25. https://doi.org/10.52294/e6198273-b8e3-4b63-babb-6e6b0da10669, PubMed: 35079748

Lebel, C., Treit, S., & Beaulieu, C. (2019). A review of diffusion MRI of typical white matter development from early childhood to young adulthood. *NMR in Biomedicine*, *32*(4), Article e3778. https://doi.org/10.1002/nbm.3778, PubMed: 28886240

Lee, H., Sim, H., Lee, E., & Choi, D. (2017). Disfluency characteristics of children with attention-deficit/hyperactivity disorder symptoms. *Journal of Communication Disorders*, *65*, 54–64. https://doi.org/10.1016/j.jcomdis.2016.12.001, PubMed: 28038762

Levelt, W. J., Roelofs, A., & Meyer, A. S. (1999). A theory of lexical access in speech production. *Behavioral and Brain Sciences*, *22*(1), 1–38. https://doi.org/10.1017/S0140525X99001776, PubMed: 11301520

Liégeois, F. J., Butler, J., Morgan, A. T., Clayden, J. D., & Clark, C. A. (2016). Anatomy and lateralization of the human corticobulbar tracts: An fMRI-guided tractography study. *Brain Structure and Function*, *221*(6), 3337–3345. https://doi.org/10.1007/s00429-015-1104-x, PubMed: 26411871

Liégeois, F. [J.], Tournier, J.-D., Pigdon, L., Connelly, A., & Morgan, A. T. (2013). Corticobulbar tract changes as predictors of dysarthria in childhood brain injury. *Neurology*, *80*(10), 926–932. https://doi.org/10.1212/WNL.0b013e3182840c6d, PubMed: 23390172

Liégeois, F. J., Turner, S. J., Mayes, A., Bonthrone, A. F., Boys, A., Smith, L., Parry-Fielder, B., Mandelstam, S., Spencer-Smith, M., Bahlo, M., Scerri, T. S., Hildebrand, M. S., Scheffer, I. E., Connelly, A., & Morgan, A. T. (2019). Dorsal language stream anomalies in an inherited speech disorder. *Brain*, *142*(4), 966–977. https://doi.org/10.1093/brain/awz018, PubMed: 30796815

Lu, J., Zhao, Z., Zhang, J., Wu, B., Zhu, Y., Chang, E. F., Wu, J., Duffau, H., & Berger, M. S. (2021). Functional maps of direct electrical stimulation-induced speech arrest and anomia: A multicentre retrospective study. *Brain*, *144*(8), 2541–2553. https://doi.org/10.1093/brain/awab125, PubMed: 33792674

Mandelli, M. L., Caverzasi, E., Binney, R. J., Henry, M. L., Lobach, I., Block, N., Amirbekian, B., Dronkers, N., Miller, B. L., Henry, R. G., & Gorno-Tempini, M. L. (2014). Frontal white matter tracts sustaining speech production in primary progressive aphasia. *Journal of Neuroscience*, *34*(29), 9754–9767. https://doi.org/10.1523/JNEUROSCI.3464-13.2014, PubMed: 25031413

McGrath, L. M., Hutaff-Lee, C., Scott, A., Boada, R., Shriberg, L. D., & Pennington, B. F. (2008). Children with comorbid speech sound disorder and specific language impairment are at increased risk for attention-deficit/hyperactivity disorder. *Journal of Abnormal Child Psychology*, *36*(2), 151–163. https://doi.org/10.1007/s10802-007-9166-8, PubMed: 17882543

Misaghi, E., Zhang, Z., Gracco, V. L., De Nil, L. F., & Beal, D. S. (2018). White matter tractography of the neural network for speech-motor control in children who stutter. *Neuroscience Letters*, *668*, 37–42. https://doi.org/10.1016/j.neulet.2018.01.009, PubMed: 29309858

Morgan, A. T., Liégeois, F., Liederkerke, C., Vogel, A. P., Hayward, R., Harkness, W., Chong, K., & Vargha-Khadem, F. (2011). Role of cerebellum in fine speech control in childhood: Persistent dysarthria after surgical treatment for posterior fossa tumour. *Brain and Language*, *117*(2), 69–76. https://doi.org/10.1016/j.bandl.2011.01.002, PubMed: 21334735

Morgan, A. T., Su, M., Reilly, S., Conti-Ramsden, G., Connelly, A., & Liégeois, F. J. (2018). A brain marker for developmental speech disorders. *Journal of Pediatrics*, *198*, 234–239. https://doi.org/10.1016/j.jpeds.2018.02.043, PubMed: 29705112

Morgan, P. S., Bowtell, R. W., McIntyre, D. J., & Worthington, B. S. (2004). Correction of spatial distortion in EPI due to inhomogeneous static magnetic fields using the reversed gradient method.

Journal of Magnetic Resonance Imaging, *19*(4), 499–507. https://doi.org/10.1002/jmri.20032, PubMed: 15065175

Mueller, K. L., & Tomblin, J. B. (2012). Examining the comorbidity of language impairment and attention-deficit/hyperactivity disorder. *Topics in Language Disorders*, *32*(3), 228–246. https://doi.org/10.1097/TLD.0b013e318262010d, PubMed: 25505812

Muncy, N. M., Kimbler, A., Hedges-Muncy, A. M., McMakin, D. L., & Mattfeld, A. T. (2022). General additive models address statistical issues in diffusion MRI: An example with clinically anxious adolescents. *NeuroImage: Clinical*, *33*, Article 102937. https://doi.org/10.1016/j.nicl.2022.102937, PubMed: 35033812

Nagahama, H., Wanibuchi, M., Hirano, T., Nakanishi, M., & Takashima, H. (2021). Visualization of cerebellar peduncles using diffusion tensor imaging. *Acta Neurochirurgica*, *163*(3), 619–624. https://doi.org/10.1007/s00701-020-04511-6, PubMed: 32728902

Naidich, T. P., Duvernoy, H. M., Delman, B. N., Sorensen, A. G., Kollias, S. S., & Haacke, E. M. (2009). *Duvernoy's atlas of the human brain stem and cerebellum: High-field MRI, surface anatomy, internal structure, vascularization and 3D sectional anatomy*. Springer. https://doi.org/10.1007/978-3-211-73971-6

Northam, G. B., Morgan, A. T., Fitzsimmons, S., Baldeweg, T., & Liégeois, F. J. (2019). Corticobulbar tract injury, oromotor impairment and language plasticity in adolescents born preterm. *Frontiers in Human Neuroscience*, *13*, Article 45. https://doi.org/10.3389/fnhum.2019.00045, PubMed: 30837853

Oberhuber, M., Hope, T. M. H., Seghier, M. L., Parker Jones, O., Prejawa, S., Green, D. W., & Price, C. J. (2016). Four functionally distinct regions in the left supramarginal gyrus support word processing. *Cerebral Cortex*, *26*(11), 4212–4226. https://doi.org/10.1093/cercor/bhw251, PubMed: 27600852

Oldfield, R. C. (1971). The assessment and analysis of handedness: The Edinburgh inventory. *Neuropsychologia*, *9*(1), 97–113. https://doi.org/10.1016/0028-3932(71)90067-4, PubMed: 5146491

Olulade, O. A., Seydell-Greenwald, A., Chambers, C. E., Turkeltaub, P. E., Dromerick, A. W., Berl, M. M., Gaillard, W. D., & Newport, E. L. (2020). The neural basis of language development: Changes in lateralization over age. *Proceedings of the National Academy of Sciences*, *117*(38), 23477–23483. https://doi.org/10.1073/pnas.1905590117, PubMed: 32900940

Palmer, C. E., Pecheva, D., Iversen, J. R., Hagler, D. J., Jr., Sugrue, L., Nedelec, P., Fan, C. C., Thompson, W. K., Jernigan, T. L., & Dale, A. M. (2022). Microstructural development from 9 to 14 years: Evidence from the ABCD study. *Developmental Cognitive Neuroscience*, *53*, Article 101044. https://doi.org/10.1016/j.dcn.2021.101044, PubMed: 34896850

Parekh, P., Fan, C. C., Frei, O., Palmer, C. E., Smith, D. M., Makowski, C., Iversen, J. R., Pecheva, D., Holland, D., Loughnan, R., Nedelec, P., Thompson, W. K., Hagler, D. J., Jr., Andreassen, O. A., Jernigan, T. L., Nichols, T. E., & Dale, A. M. (2024). FEMA: Fast and efficient mixed-effects algorithm for large sample whole-brain imaging data. *Human Brain Mapping*, *45*(2), Article e26579. https://doi.org/10.1002/hbm.26579, PubMed: 38339910

Peeva, M. G., Guenther, F. H., Tourville, J. A., Nieto-Castanon, A., Anton, J.-L., Nazarian, B., & Alario, F.-X. (2010). Distinct representations of phonemes, syllables, and supra-syllabic sequences in the speech production network. *NeuroImage*, *50*(2), 626–638. https://doi.org/10.1016/j.neuroimage.2009.12.065, PubMed: 20035884

Pelham, W. E., Jr., Gnagy, E. M., Greenslade, K. E., & Milich, R. (1992). Teacher ratings of DSM-III-R symptoms for the disruptive behavior disorders. *Journal of the American Academy of Child and Adolescent Psychiatry*, *31*(2), 210–218. https://doi.org/10.1097/00004583-199203000-00006, PubMed: 1564021

Pigdon, L., Willmott, C., Reilly, S., Conti-Ramsden, G., Liegeois, F., Connelly, A., & Morgan, A. T. (2020). The neural basis of nonword repetition in children with developmental speech or language disorder: An fMRI study. *Neuropsychologia*, *138*, Article 107312. https://doi.org/10.1016/j.neuropsychologia.2019.107312, PubMed: 31917203

Pigdon, L., Willmott, C., Reilly, S., Conti-Ramsden, G., & Morgan, A. T. (2020). What predicts nonword repetition performance? *Child Neuropsychology*, *26*(4), 518–533. https://doi.org/10.1080/09297049.2019.1674799, PubMed: 31581884

Rauschecker, J. P. (1998). Cortical processing of complex sounds. *Current Opinion in Neurobiology*, *8*(4), 516–521. https://doi.org/10.1016/S0959-4388(98)80040-8, PubMed: 9751652

Rauschecker, J. P., & Scott, S. K. (2009). Maps and streams in the auditory cortex: Nonhuman primates illuminate human speech processing. *Nature Neuroscience*, *12*(6), 718–724. https://doi.org/10.1038/nn.2331, PubMed: 19471271

Riecker, A., Kassubek, J., Gröschel, K., Grodd, W., & Ackermann, H. (2006). The cerebral control of speech tempo: Opposite relationship between speaking rate and BOLD signal changes at striatal and cerebellar structures. *NeuroImage*, *29*(1), 46–53. https://doi.org/10.1016/j.neuroimage.2005.03.046, PubMed: 16085428

Riecker, A., Mathiak, K., Wildgruber, D., Erb, M., Hertrich, I., Grodd, W., & Ackermann, H. (2005). fMRI reveals two distinct cerebral networks subserving speech motor control. *Neurology*, *64*(4), 700–706. https://doi.org/10.1212/01.WNL.0000152156.90779.89, PubMed: 15728295

Rowan, A., Vargha-Khadem, F., Calamante, F., Tournier, J.-D., Kirkham, F. J., Chong, W. K., Baldeweg, T., Connelly, A., & Gadian, D. G. (2007). Cortical abnormalities and language function in young patients with basal ganglia stroke. *NeuroImage*, *36*(2), 431–440. https://doi.org/10.1016/j.neuroimage.2007.02.051, PubMed: 17462915

Rvachew, S., & Matthews, T. (2017). Using the Syllable Repetition Task to reveal underlying speech processes in childhood apraxia of speech: A tutorial. *Canadian Journal of Speech-Language Pathology and Audiology*, *41*(1), 106–126.

Sagi, Y., Tavor, I., Hofstetter, S., Tzur-Moryosef, S., Blumenfeld-Katzir, T., & Assaf, Y. (2012). Learning in the fast lane: New insights into neuroplasticity. *Neuron*, *73*(6), 1195–1203. https://doi.org/10.1016/j.neuron.2012.01.025, PubMed: 22445346

Sarıyer, M. N., Tadıhan Özkan, E., & Fidan, S. T. (2023). The relationship between speech and language disorders and working memory: Children with attention deficit and hyperactivity disorder and typical development. *Journal of Attention Disorders*, *27*(12), 1420–1430. https://doi.org/10.1177/10870547231177236, PubMed: 37254477

Schilling, K. G., Blaber, J., Hansen, C., Cai, L., Rogers, B., Anderson, A. W., Smith, S., Kanakaraj, P., Rex, T., Resnick, S. M., Shafer, A. T., Cutting, L. E., Woodward, N., Zald, D., & Landman, B. A. (2020). Distortion correction of diffusion weighted MRI without reverse phase-encoding scans or field-maps. *PLOS ONE*, *15*(7), Article e0236418. https://doi.org/10.1371/journal.pone.0236418, PubMed: 32735601

Schilling, K. G., Blaber, J., Huo, Y., Newton, A., Hansen, C., Nath, V., Shafer, A. T., Williams, O., Resnick, S. M., Rogers, B., Anderson, A. W., & Landman, B. A. (2019). Synthesized b0 for diffusion distortion correction (Synb0-DisCo). *Magnetic Resonance Imaging*, *64*, 62–70. https://doi.org/10.1016/j.mri.2019.05.008, PubMed: 31075422

Schlösser, R., Hutchinson, M., Joseffer, S., Rusinek, H., Saarimaki, A., Stevenson, J., Dewey, S., & Brodie, J. D. (1998). Functional magnetic resonance imaging of human brain activity in a verbal fluency task. *Journal of Neurology, Neurosurgery, and Psychiatry, 64*(4), 492–498. https://doi.org/10.1136/jnnp.64.4.492, PubMed: 9576541

Schweizer, T. A., Alexander, M. P., Gillingham, B. A. S., Cusimano, M., & Stuss, D. T. (2010). Lateralized cerebellar contributions to word generation: A phonemic and semantic fluency study. *Behavioural Neurology, 23*(1–2), 31–37. https://doi.org/10.3233/BEN-2010-0269, PubMed: 20714059

Shaffer, D., Fisher, P., Lucas, C. P., Dulcan, M. K., & Schwab-Stone, M. E. (2000). NIMH Diagnostic Interview Schedule for Children Version IV (NIMH DISC-IV): Description, differences from previous versions, and reliability of some common diagnoses. *Journal of the American Academy of Child and Adolescent Psychiatry, 39*(1), 28–38. https://doi.org/10.1097/00004583-200001000-00014, PubMed: 10638065

Shriberg, L. D., & Lohmeier, H. L. (2008). *The Syllable Repetition Task (SRT)* [Technical Report No. 14]. Phonology Project, Waisman Center, University of Wisconsin-Madison.

Shriberg, L. D., Lohmeier, H. L., Campbell, T. F., Dollaghan, C. A., Green, J. R., & Moore, C. A. (2009). A nonword repetition task for speakers with misarticulations: The Syllable Repetition Task (SRT). *Journal of Speech, Language, and Hearing Research, 52*(5), 1189–1212. https://doi.org/10.1044/1092-4388(2009/08-0047), PubMed: 19635944

Shuster, L. I., & Lemieux, S. K. (2005). An fMRI investigation of covertly and overtly produced mono-and multisyllabic words. *Brain and Language, 93*(1), 20–31. https://doi.org/10.1016/j.bandl.2004.07.007, PubMed: 15766765

Stoodley, C. J., Valera, E. M., & Schmahmann, J. D. (2012). Functional topography of the cerebellum for motor and cognitive tasks: An fMRI study. *NeuroImage, 59*(2), 1560–1570. https://doi.org/10.1016/j.neuroimage.2011.08.065, PubMed: 21907811

Tisdall, M. D., Hess, A. T., Reuter, M., Meintjes, E. M., Fischl, B., & van der Kouwe, A. J. W. (2012). Volumetric navigators for prospective motion correction and selective reacquisition in neuroanatomical MRI. *Magnetic Resonance in Medicine, 68*(2), 389–399. https://doi.org/10.1002/mrm.23228, PubMed: 22213578

Tomblin, J. B., & Mueller, K. L. (2012). How can comorbidity with attention-deficit/hyperactivity disorder aid understanding of language and speech disorders? *Topics in Language Disorders, 32*(3), 198–206. https://doi.org/10.1097/TLD.0b013e318261c264, PubMed: 24817779

Tremblay, P., & Dick, A. S. (2016). Broca and Wernicke are dead, or moving past the classic model of language neurobiology. *Brain and Language, 162*, 60–71. https://doi.org/10.1016/j.bandl.2016.08.004, PubMed: 27584714

Tremblay, P., & Gracco, V. L. (2009). Contribution of the pre-SMA to the production of words and non-speech oral motor gestures, as revealed by repetitive transcranial magnetic stimulation (rTMS). *Brain Research, 1268*, 112–124. https://doi.org/10.1016/j.brainres.2009.02.076, PubMed: 19285972

Tremblay, P., & Gracco, V. L. (2010). On the selection of words and oral motor responses: Evidence of a response-independent fronto-parietal network. *Cortex, 46*(1), 15–28. https://doi.org/10.1016/j.cortex.2009.03.003, PubMed: 19362298

Turkeltaub, P. E., Eden, G. F., Jones, K. M., & Zeffiro, T. A. (2002). Meta-analysis of the functional neuroanatomy of single-word reading: Method and validation. *NeuroImage, 16*(3A), 765–780. https://doi.org/10.1006/nimg.2002.1131, PubMed: 12169260

Urban, P. P., Marx, J., Hunsche, S., Gawehn, J., Vucurevic, G., Wicht, S., Massinger, C., Stoeter, P., & Hopf, H. C. (2003). Cerebellar speech representation: Lesion topography in dysarthria as derived from cerebellar ischemia and functional magnetic resonance imaging. *Archives of Neurology, 60*(7), 965–972. https://doi.org/10.1001/archneur.60.7.965, PubMed: 12873853

Vassal, F., Boutet, C., Lemaire, J.-J., & Nuti, C. (2014). New insights into the functional significance of the frontal aslant tract: An anatomo–functional study using intraoperative electrical stimulations combined with diffusion tensor imaging-based fiber tracking. *British Journal of Neurosurgery, 28*(5), 685–687. https://doi.org/10.3109/02688697.2014.889810, PubMed: 24552256

Vias, C., & Dick, A. S. (2017). Cerebellar contributions to language in typical and atypical development: A review. *Developmental Neuropsychology, 42*(6), 404–421. https://doi.org/10.1080/87565641.2017.1334783, PubMed: 28885046

Vydrova, R., Komarek, V., Sanda, J., Sterbova, K., Jahodova, A., Maulisova, A., Zackova, J., Reissigova, J., Krsek, P., & Kyncl, M. (2015). Structural alterations of the language connectome in children with specific language impairment. *Brain and Language, 151*, 35–41. https://doi.org/10.1016/j.bandl.2015.10.003, PubMed: 26609941

Wechsler, D. (2012). *Wechsler preschool and primary scale of intelligence* (4th ed.). Pearson.

White, N. S., Leergaard, T. B., D'Arceuil, H., Bjaalie, J. G., & Dale, A. M. (2013). Probing tissue microstructure with restriction spectrum imaging: Histological and theoretical validation. *Human Brain Mapping, 34*(2), 327–346. https://doi.org/10.1002/hbm.21454, PubMed: 23169482

White, N. S., McDonald, C. R., Farid, N., Kuperman, J. M., Kesari, S., & Dale, A. M. (2013). Improved conspicuity and delineation of high-grade primary and metastatic brain tumors using "restriction spectrum imaging": Quantitative comparison with high B-value DWI and ADC. *American Journal of Neuroradiology, 34*(5), 958–964. https://doi.org/10.3174/ajnr.A3327, PubMed: 23139079

White, N. S., McDonald, C. R., Farid, N., Kuperman, J., Karow, D., Schenker-Ahmed, N. M., Bartsch, H., Rakow-Penner, R., Holland, D., Shabaik, A., Bjørnerud, A., Hope, T., Hattangadi-Gluth, J., Liss, M., Parsons, J. K., Chen, C. C., Raman, S., Margolis, D., Reiter, R. E., … Dale, A. M. (2014). Diffusion-weighted imaging in cancer: Physical foundations and applications of restriction spectrum imaging. *Cancer Research, 74*(17), 4638–4652. https://doi.org/10.1158/0008-5472.CAN-13-3534, PubMed: 25183788

Willems, R. M., Özyürek, A., & Hagoort, P. (2009). Differential roles for left inferior frontal and superior temporal cortex in multimodal integration of action and language. *NeuroImage, 47*(4), 1992–2004. https://doi.org/10.1016/j.neuroimage.2009.05.066, PubMed: 19497376

Yablonski, M., Menashe, B., & Ben-Shachar, M. (2021). A general role for ventral white matter pathways in morphological processing: Going beyond reading. *NeuroImage, 226*, Article 117577. https://doi.org/10.1016/j.neuroimage.2020.117577, PubMed: 33221439

Yeatman, J. D., Dougherty, R. F., Myall, N. J., Wandell, B. A., & Feldman, H. M. (2012). Tract profiles of white matter properties: Automating fiber-tract quantification. *PLOS ONE, 7*(11), Article e49790. https://doi.org/10.1371/journal.pone.0049790, PubMed: 23166771

Yeatman, J. D., Dougherty, R. F., Rykhlevskaia, E., Sherbondy, A. J., Deutsch, G. K., Wandell, B. A., & Ben-Shachar, M. (2011). Anatomical properties of the arcuate fasciculus predict phonological and reading skills in children. *Journal of Cognitive Neuroscience*, *23*(11), 3304–3317. https://doi.org/10.1162/jocn_a_00061, PubMed: 21568636

Yendiki, A., Koldewyn, K., Kakunoori, S., Kanwisher, N., & Fischl, B. (2014). Spurious group differences due to head motion in a diffusion MRI study. *NeuroImage*, *88*, 79–90. https://doi.org/10.1016/j.neuroimage.2013.11.027, PubMed: 24269273

Zhang, H., Schneider, T., Wheeler-Kingshott, C. A., & Alexander, D. C. (2012). NODDI: Practical *in vivo* neurite orientation dispersion and density imaging of the human brain. *NeuroImage*, *61*(4), 1000–1016. https://doi.org/10.1016/j.neuroimage.2012.03.072, PubMed: 22484410

Zhong, A. J., Baldo, J. V., Dronkers, N. F., & Ivanova, M. V. (2022). The unique role of the frontal aslant tract in speech and language processing. *NeuroImage: Clinical*, *34*, Article 103020. https://doi.org/10.1016/j.nicl.2022.103020, PubMed: 35526498